

The concentration-discharge slope as a tool for water quality management

M.Z. Bieroza¹, A.L. Heathwaite², M. Bechmann³, K. Kyllmar¹ and P. Jordan⁴

¹Department of Soil and Environment, Swedish University of Agricultural Sciences, Uppsala, Box 7014, 750 07, Sweden, magdalena.bieroza@slu.se, katarina.kyllmar@slu.se

²Lancaster Environment Centre, Library Avenue, Lancaster University, Lancaster LA1 4YQ, United Kingdom, louise.heathwaite@lancaster.ac.uk

³Norwegian Institute of Bioeconomy Research, P.O. Box 115, NO-1431 Ås, Norway, marianne.bechmann@nibio.no

⁴School of Geography & Environmental Sciences, Ulster University, Coleraine, BT52 1SA, United Kingdom, p.jordan@ulster.ac.uk

Abstract

Recent technological breakthroughs of optical sensors and analysers have enabled matching the water quality measurement interval to the time scales of stream flow changes and led to an improved understanding of spatially and temporally heterogeneous sources and delivery pathways for many solutes and particulates. This new ability to match the chemograph with the hydrograph has promoted renewed interest in the concentration-discharge ($c-q$) relationship and its value in characterising catchment storage, time lags and legacy effects for both weathering products and anthropogenic pollutants. In this paper we evaluated the stream $c-q$ relationships for a number of water quality determinands (phosphorus, suspended sediments, nitrogen) in intensively managed agricultural catchments based on both high-frequency (sub-hourly) and long-term low-frequency (fortnightly-monthly) routine monitoring data. We used resampled high-frequency data to test the uncertainty in water quality parameters (e.g. mean, 95th percentile and load) derived from low-frequency sub-datasets. We showed that the uncertainty in water quality parameters increases with reduced sampling frequency as a function of the $c-q$ slope. We also showed that different sources and delivery pathways control $c-q$

25 relationship for different solutes and particulates. Secondly, we evaluated the variation in $c-q$ slopes
26 derived from the long-term low-frequency data for different determinands and catchments and showed
27 strong chemostatic behaviour for phosphorus and nitrogen due to saturation and agricultural legacy
28 effects. The $c-q$ slope analysis can provide an effective tool to evaluate the current monitoring networks
29 and the effectiveness of water management interventions. This research highlights how improved
30 understanding of solute and particulate dynamics obtained with optical sensors and analysers can be
31 used to understand patterns in long-term water quality time series, reduce the uncertainty in the
32 monitoring data and to manage eutrophication in agricultural catchments.

33 **Keywords**

34 Eutrophication; Concentration-discharge relationship; Chemostatic behaviour; High-frequency
35 monitoring; Long-term water quality time series; Phosphorus and Nitrogen

36 **Highlights**

37 High-frequency data help to understand the patterns in long-term data
38 Chemostatic responses lead to low errors in water quality parameters
39 Low-order agricultural catchments homogenize stream solute responses
40 Phosphorus and nitrogen chemostatic responses are driven by legacy stores
41 Concentration-discharge slope helps to prioritise monitoring and mitigation efforts

42 **Introduction**

43 Combating eutrophication is proving difficult and exposes gaps in our scientific understanding of
44 hydrological and biogeochemical processes controlling stream concentrations of solutes and
45 particulates. The relative importance of these processes and contribution of dominant sources and
46 delivery pathways is captured by the concentration-discharge ($c-q$) relationship. The $c-q$ relationship
47 characterises solute/particulate change (dilution or concentration) with varying flow (Evans and Davies,
48 1998) and can be quantified as the slope b of the $c-q$ regression relationship on logarithmic axes (Godsey

49 et al., 2009). The c - q relationship is often complex due to hydrochemical variability but can generally
50 be classified into two patterns: chemostatic ($|b| < 0.1$) and chemodynamic ($|b| > 0.1$) with either dilution
51 ($b < -0.1$) or concentration ($b > 0.1$) pattern. The chemostatic c - q pattern, in which the concentrations are
52 stable over a large range of flows has been observed for many solutes and particulates with an abundant
53 source of the chemical in the catchment (Thompson et al., 2011) e.g. weathering bedrock (Ameli et al.,
54 2017; Godsey et al., 2009; Hoagland et al., 2017) or agricultural soils and the unsaturated zone (Basu
55 et al., 2011; Van Meter et al., 2017). These sources are also referred to as the legacy stores that can
56 control the mobilisation and stream transport of the chemicals in the long-term and lead to transport-
57 limitation (Basu et al., 2011). When the rate of the concentration change is larger than the flow change,
58 a chemodynamic c - q pattern and source-limitation are observed with either concentrations increasing
59 (concentration) or decreasing (dilution). Recent increased availability of high-frequency (sub-hourly) c
60 and q data, due to deployment of optical sensors and wet-chemistry analysers, has led to improved
61 understanding of the complex c - q patterns observed in water quality data. For example, recent work
62 explains how both seasonal and storm-to-storm dynamics in source mobilisation and activation of
63 different delivery pathways control the chemostatic and chemodynamic c - q responses (Bieroza and
64 Heathwaite, 2015; Lloyd et al., 2016).

65 To date, the c - q relationship has been evaluated for a large range of chemicals both derived from
66 weathering of bedrock and from agricultural land use. The studies of c - q dynamics in agricultural
67 catchments focus on chemicals that are of major concern due to increasing eutrophication and hypoxia
68 of inland and coastal waters: phosphorus (P) both as total P (TP) and total and soluble reactive P (TRP
69 and SRP) (Basu et al., 2011; Bieroza and Heathwaite, 2015; Dupas et al., 2015), suspended sediments
70 (SS) measured directly or with turbidity (TURB) as a proxy (Lawler et al., 2006), organic and inorganic
71 nitrogen (N), particularly in the form of nitrate-nitrogen ($\text{NO}_3\text{-N}$) (Bieroza et al., 2014; Dupas et al.,
72 2016; Van Meter et al., 2017) and compounds that provide information on the general hydrochemical
73 functioning of catchments: total and dissolved organic carbon (TOC and DOC) (Butturini et al., 2008;
74 Hoagland et al., 2017) and specific conductivity (COND) (Bieroza and Heathwaite, 2015) .

75 Hydrochemical data have been collected for over 150 years (Howden et al., 2010) and most of these
76 long-term datasets are from rivers (>4th Strahler order) and collected at low frequency (typically
77 monthly) (Tetzlaff et al., 2017). Therefore, this existing water quality sampling method is not suited to
78 target the highly variable, in space and time, agricultural P and N pollution in low-order (<3rd Strahler
79 order) catchments (Bieroza et al., 2014). Recent advances in *in situ* water quality monitoring with
80 optical sensors and wet-chemistry analysers (Bieroza and Heathwaite, 2016; Flourey et al., 2017; Jordan
81 et al., 2012; Rode et al., 2016) help to bridge this gap, but due to high-financial cost of the *in situ*
82 technology per sampling site, new approaches that integrate the high- and low-frequency sampling are
83 needed (Bieroza et al., 2014; Chappell et al., 2017; Jordan and Cassidy, 2011). To address this scientific
84 and management need, we propose that the new knowledge of *c-q* dynamics obtained with high-
85 frequency sampling can improve the understanding of hydrochemical patterns in readily available long-
86 term datasets and can help to prioritise monitoring and mitigation efforts.

87 Specifically, we evaluated the uncertainty and variation in the *c-q* relationship for selected solutes and
88 particulates, for a number of low-order small agricultural catchments in the UK, Norway and Sweden
89 that are subjected to eutrophication pressures. We hypothesized that the *c-q* slope represents the
90 catchment's tendency to store and transport chemicals and that it can be a useful tool in water
91 management practice. Our objectives were to: **1)** evaluate the variation in the *c-q* slopes for P, SS, NO₃-
92 N, DOC and COND for both high- and low-frequency sampling, **2)** evaluate the uncertainty in
93 operational water quality parameters (mean, 95th percentile and load) derived from low-frequency
94 datasets as a function of the *c-q* slope, **3)** provide recommendations on how the *c-q* slopes can help to
95 improve water quality management.

96 **Methods**

97 *High-frequency datasets*

98 Two high-frequency datasets were used in the analysis: HF1 (Leith catchment, UK, 2009-2014, hourly
99 and sub-hourly, TP, TRP, TURB, NO₃-N and COND) and HF2 (SE3 catchment, SE, 2017-2018, sub-
100 hourly, TP, TRP, TURB, NO₃-N and DOC) with continuous flow discharge measurements. Similar

101 experimental setups were deployed in both cases, with stream water pumped to a small hut on the bank
102 and the measurements conducted on unfiltered samples with wet-chemistry analysers (Systea's Micro
103 Mac for HF1 and Hach Lange's Phosphax for HF2 giving TP and TRP) and in-line optical sensors for
104 TURB and solutes (Systea's WaterWatch and Hach Lange's Nitratex for HF1 and s:can's Spectrolyser
105 for HF2). The details of the HF1 experimental setup and principles of the *in situ* monitoring are given
106 elsewhere (Bieroza and Heathwaite, 2015; Bieroza and Heathwaite, 2016; Bieroza et al., 2014). Both
107 study catchments represent small, low-order catchments dominated by agricultural land use: grassland
108 and livestock grazing in the Leith catchment (HF1 in Table 1) and arable land and crop production in
109 the SE3 catchment (HF2 in Table 1). The catchments differ in terms of geology and soils, with sandstone
110 and loam soils in HF1 and marine clay and heavy clay soils in HF2 with the effect on hydrology:
111 intensive ground-surface water interactions (Krause et al., 2009) and subsurface flow pathways in HF1
112 (Bieroza et al., 2014) and overland, macropore and tile drainage flow pathways in HF2 (Ulén et al.,
113 2011).

114 *Low-frequency datasets*

115 We collated long-term low-frequency water quality time series (TP, TRP and SRP, SS, NO₃-N, DOC
116 and TOC and COND) for agricultural catchments subject to risk of eutrophication from three EU
117 countries (UK, Norway and Sweden) spanning a range of climatic and soil conditions (USDA, 1987)
118 (Table 1). The datasets varied in terms of sampling frequency: fortnightly sampling for the Swedish and
119 Norwegian catchments under Agricultural Monitoring Programmes to 6-12 samples a year in the UK
120 catchments under the routine monitoring programmes (Water Framework and Nitrates Directives).

121 In the UK, all environmental datasets were accessed online: the water quality datasets were obtained
122 from the Environment Agency (<http://environment.data.gov.uk/water-quality>), flow records from the
123 National River Flow Archive (<https://nrfa.ceh.ac.uk/>) and soil data from the UK Soil Observatory Map
124 (<http://www.ukso.org/home.html>). As the UK does not have a specific agricultural impact monitoring
125 programme, unlike Sweden and Norway, a selection of the sampling points and study catchments was
126 made from over 1500 gauging stations and over 7000 water quality sampling points with the following

127 criteria: continuous (no breaks due to gauging station closure) flow discharge record, catchment area
128 <60 km², agricultural land use >70%, no major settlements/fish farms/sewage treatment outlets in the
129 catchment and a nearby water quality sampling point (up to 50 m upstream and 100 m downstream,
130 with no tributaries between both points) with at least 50 TRP and NO₃-N measurements. Based on these
131 criteria, a selection of 42 catchments representing diverse soil, climatic and agricultural conditions was
132 made (Table 1). For the UK, DOC and TP measurements are not part of the routine monitoring (Table
133 ST1).

134 In Norway, data about water quality and agricultural production are collected in the Agricultural
135 Environmental Monitoring Programme (JOVA) (Bechmann et al., 2008). The selected ten catchments
136 represent the main agricultural production systems in Norway including cereals (E), vegetables (S),
137 intensive dairy farming (W) and more extensive grass production (S and N) and vary in terms of soils,
138 topography and climate (Table 1). In all catchments, fortnightly flow-proportional samples are collected
139 (TP, SRP, SS, NO₃-N) and water level is recorded automatically. Since the P, SS and NO₃-N
140 concentrations and loads are high, economic subsidies and information campaigns have been introduced
141 to reduce pollution through e.g. reduction in autumn ploughing, improved nutrient and animal waste
142 management and mitigation measures (buffer zones and constructed wetlands) (Bechmann et al., 2008).

143 In Sweden, ten small agricultural catchments (Table 1) have been monitored for agricultural impact on
144 water quality for more than 20 years (Kyllmar et al., 2014). Fortnightly water quality sampling includes
145 time-proportional grab sampling (1990-2010) and flow-proportional composite sampling (from 2005)
146 for TP, TRP, SRP, NO₃-N, SS, DOC and COND with continuous flow discharge measurements. The
147 catchments represent various types of soils, agricultural production and climate with a clear
148 precipitation gradient between SW and E Sweden. Higher precipitation in the SW catchments results in
149 higher flow discharge and nutrient loads (SE6, SE8 and SE9) compared to the E catchments (SE1, SE2,
150 SE3 and SE5). As a result, the SW Sweden catchments have climatic and hydrological conditions
151 similar to the UK and Norway (Table 1). Catchments with high clay content (SE9, SE10) generally
152 have higher P and SS loads compared to those with sandy soils (SE8).

153 *Data analyses*

154 All high- and low-frequency datasets were quality controlled to remove outliers and calculate basic
155 descriptive statistics (Tables 2 and ST1). Flow discharge records were used to calculate the flashiness
156 index as a ratio of the high (5th percentile) and low flows (95th percentile) which describes the dominant
157 flow pathways in the catchment (Jordan et al., 2005). A higher flashiness index (Q5:Q95; Table 1)
158 indicates a higher ratio of flashier, faster flow responses to rainfall compared to slower, low flows
159 (baseflow and slow subsurface). For each high-frequency dataset, loads were calculated using a
160 standard algorithm based on instantaneous concentration and flow discharge (Bieroza et al., 2014;
161 Jordan and Cassidy, 2011) (Equation 1):

$$162 \quad L = \frac{K \sum_{i=1}^n C_i Q_i}{\sum_{i=1}^n Q_i} Q_T \quad (\text{Equation 1})$$

163 Where: C_i and Q_i are instantaneous high-frequency concentration and discharge data, L is the load
164 estimate, Q_T is the average flow discharge based on the long-term data, K is a constant which accounts
165 for the duration of the record, n is the number of concentration measurements.

166 To examine the effect of sampling frequency on the uncertainty in water quality parameters routinely
167 used for water management (mean, standard deviation, maximum and 95th percentile concentration,
168 load and c - q slope), the high-frequency datasets were resampled using 10,000 Monte Carlo iterations
169 each, to simulate daily, weekly, fortnightly and monthly sampling frequencies, respectively (Table 2).
170 For each simulated frequency (daily, weekly, fortnightly and monthly) 10,000 individual datasets were
171 created by randomly selecting samples from the high-frequency data with the single constraint criterion
172 – samples need to represent unique days, weeks, fortnights or months respectively. We calculated the
173 relative errors e for each water quality parameter and determinand (TP, TRP, TURB, NO₃-N, DOC and
174 COND) as Equation 2:

$$175 \quad e = \frac{100(LF-HF)}{HF} \% \quad (\text{Equation 2})$$

176 with an assumption that the high-frequency value HF (e.g. mean concentration or load) represents the
177 true value compared to the low-frequency value LF (Supplementary Tables ST2-7 and Supplementary

178 Figures SF1-3). The c - q slopes were calculated by fitting a linear regression to the log-transformed
179 concentration and flow discharge data. To compare the differences in mean errors, concentrations and
180 c - q slopes between the catchments and determinands, a non-parametric analysis of variance was used
181 (Kruskal-Wallis test). To analyse the catchment controls (e.g. soil type and flashiness) on the c - q slopes
182 and interactions between different determinands, a multivariate non-parametric canonical redundancy
183 analysis (RDA) was performed (Bieroza and Heathwaite, 2015; Legendre and Legendre, 1998).
184 Spearman's correlations p -values were corrected for multiple comparisons with a Bonferroni correction
185 (Holm, 1978) and for all analyses a uniform significance level of 0.05 was used. All data processing
186 and statistical analyses were carried out in MATLAB version 8.6 (R2015b).

187 **Results**

188 *Concentration-discharge relationship for the high-frequency datasets*

189 Comparison of the c - q relationships from the two high-frequency datasets (HF1 and HF2) showed that
190 concentration effect ($b > 0$) was predominant for both datasets with the exception of solutes: $\text{NO}_3\text{-N}_{\text{HF1}}$,
191 COND_{HF1} and TRP_{HF2} , all showing the dilution pattern ($b < 0$; Figure 1). Three determinands ($\text{NO}_3\text{-N}_{\text{HF1}}$,
192 COND_{HF1} and TP_{HF2}) showed chemostatic behaviour ($|b| < 0.1$) suggesting a predominant transport-
193 limitation mechanism (Basu et al., 2011). TP_{HF1} , TURB_{HF1} and TURB_{HF2} showed chemodynamic
194 behaviour ($|b| > 0.1$) and source-limitation mechanism ($b = 0.36, 0.27$ and 0.32). Two solutes ($\text{NO}_3\text{-N}_{\text{HF2}}$
195 and DOC_{HF2}) showed a step change from chemostatic ($b = 0.1$ and 0.04) to chemodynamic behaviour
196 ($b = 0.28$ and 0.25) at $q = 0.01 \text{ m}^3\text{s}^{-1}$ (Figure 1 and Table ST8). The c - q relationship for COND_{HF1} showed
197 non-linear curvature with two linear slopes fitted: $b = -0.06$ for flows $0\text{-}10 \text{ m}^3\text{s}^{-1}$ and $b = -0.26$ for flows
198 $> 10 \text{ m}^3\text{s}^{-1}$ (Table ST8).

199 The HF1 determinands (TP, TRP and TURB) showed a large scatter in the data due to seasonal and
200 storm-to-storm variation in the c - q behaviour and hysteretic responses (Bieroza and Heathwaite, 2015).
201 TP, TRP and TURB responded similarly in both study catchments, showing a concentration pattern.
202 Conversely, $\text{NO}_3\text{-N}_{\text{HF1}}$ and COND_{HF1} showed a weak dilution pattern, while $\text{NO}_3\text{-N}_{\text{HF2}}$ and DOC_{HF2}
203 showed an overall concentration pattern in HF2. The TRP c - q pattern was the opposite to solutes in

204 both datasets – a concentration pattern in HF1 similar to TP and TURB and a dilution pattern in HF2 in
205 contrast to both TP and TURB (Figure 1).

206 *Uncertainty in water quality parameters estimated from the low-frequency datasets*

207 To assess the uncertainty in derivation of water quality parameters from routine low-frequency
208 monitoring, the high-frequency datasets were resampled to simulate daily, weekly, fortnightly and
209 monthly sampling (Table 2). For all determinands, the mean and standard deviation of the resampled
210 datasets were consistent with the values derived from the high-frequency datasets (suggesting that the
211 errors were normally distributed), whereas the maximum gradually decreased with the sampling
212 frequency (Table 2).

213 In general, the uncertainty increased for all parameters and determinands with decreasing sampling
214 frequency (Tables ST2-7). The mean concentration, which is often used as an indicator of water quality
215 status, was underestimated by the low-frequency sampling for TP and TURB. The errors in the mean
216 TRP and NO₃-N concentrations showed two patterns: underestimation or both under- and over-
217 estimation (Figures 2 and SF1-3). The lowest errors (<10%) were observed for NO₃-N_{HF1} and COND_{HF1}
218 and the largest for TURB and TP with the greatest underestimations of -441% TURB_{HF2}, -305%
219 TURB_{HF1}, -288% TP_{HF2} for the monthly datasets (Table ST2). Similar patterns were seen in the errors
220 in calculation of the 95th percentile (Table ST5), instantaneous load (Table ST6) and the *c-q* slopes
221 (Table ST7). The general trend was that determinands showing near-chemostatic *c-q* slopes (NO₃-N_{HF1},
222 COND_{HF1}, TP_{HF2} and TRP_{HF2}) had lower errors for all water quality parameters compared to the
223 determinands with the chemodynamic slopes (Figures 2 and SF1-3). From all determinands, TURB
224 showed the largest errors spanning three orders of magnitude for all low-frequency sampling
225 simulations. This shows that only sub-hourly sampling can accurately capture the SS dynamics.

226 The observation that uncertainty in the water quality parameters derived from the low-frequency data
227 is low for near-zero, chemostatic slopes ($|b| < 0.1$) and high for chemodynamic *c-q* slopes ($|b| > 0.1$) can
228 be tested by plotting the mean *c-q* slope and mean parameter estimation error from 10,000 Monte Carlo
229 simulations (Figure 3). The positive correlation ($R^2=0.52$) indicates that errors are small (0-20%) for

230 the low c - q slopes and increase with the increasing c - q slopes. Solutes showed lower slopes and errors
231 and the highest values of slopes and errors were observed for both particulates and solutes. For the same
232 determinand, the slopes can be different between catchments suggesting that distribution of the delivery
233 pathways and catchment-specific processes play an important role in controlling the c - q relationship.
234 The high variation in the load estimation errors for similar values of the c - q slopes for $TURB_{HF1}$,
235 $TURB_{HF2}$ and TP_{HF2} can be seen in Figure 4. In contrast, NO_3-N_{HF1} and $COND_{HF1}$ showed very little
236 variation in the simulated c - q slopes and corresponding load estimation errors. The much wider range
237 of the observed c - q slopes for the HF2 dataset can be explained by a more flashy catchment character
238 compared to HF1 (Q5:Q95 237 to 74, Table 1). From all determinands, only the TRP_{HF2} showed a shift
239 from a strong dilution pattern ($b=-0.5$) and high load overestimation (up to 50%) to near-chemostatic
240 behaviour ($b=-0.1$) and small load estimation errors (10%, Figure 4).

241 *Variation in the c - q relationship in the low-frequency datasets*

242 To evaluate the variation in the c - q slopes for different determinands, we analysed available water
243 quality time series for selected agricultural catchments in the UK, Norway and Sweden (Tables 1 and
244 ST1). Mean concentrations (Table ST1) varied between determinands and countries (Figure 5). The
245 Norwegian and Swedish catchments showed higher TP and SS and lower TRP and NO_3-N
246 concentrations compared to the UK catchments. These differences result from different dominant
247 geology and soil types: post-glacial clay geology and fine texture soils in the Norwegian and Swedish
248 catchments (Kyllmar et al., 2014) with a high risk of TP and SS losses and permeable sediments with
249 deep unsaturated zone in the UK catchments (Ascott et al., 2016) with a high risk of NO_3-N and TRP
250 pollution (Bieroza et al., 2014).

251 Figure 6 shows the variation in the c - q slopes between determinands. TRP showed the largest variation
252 with the c - q slopes from $b=-0.6$ (strong dilution pattern) to $b=0.5$ (strong concentration pattern). Two
253 solutes, DOC and COND showed a typical chemostatic c - q behaviour with near-zero slope b values (-
254 0.08 and 0.08 respectively) and a small variation in the c - q relationship. The SS concentrations showed
255 a predominant concentration pattern (mean $b=0.40$) with slopes changing between -0.1 and 0.9, while

256 both TP and NO₃-N exhibited a weak chemostatic/concentration pattern (mean $b=0.12$ and 0.18
257 respectively). For the TP concentrations, the predominant type of the $c-q$ relationship measured as a
258 single slope b will depend on the relative contribution of particulate and dissolved fractions of P. This
259 effect can be seen in Figure 1; for HF1 both the TP and TRP show similar $c-q$ slopes as the TRP/TP
260 ratio is 85% but for HF2 (TRP/TP ratio is 60%) the TP slope is almost the arithmetic mean of the SS
261 (TURB) and TRP slopes. This averaging of the particulate and solute $c-q$ behaviour for the TP results
262 in near-chemostatic behaviour for analysed agricultural catchments.

263 To evaluate the effect of catchment properties (Table 1) and mean determinand concentrations (Table
264 ST1) on the observed $c-q$ slopes, we conducted a redundancy analysis (Figure 7). The catchment
265 properties explained 57% of the variance in the $c-q$ slopes of TRP, SS and NO₃-N, with the b_{TRP}
266 positively correlated with the first canonical axis and b_{SS} negatively and b_{NO_3-N} positively correlated with
267 the second canonical axis. No significant effects of the catchment area, percentage of the agricultural
268 land use or Strahler order were observed since our study explicitly focuses on low order, small
269 agricultural catchments. The first canonical axis discriminated between catchments with high TRP
270 concentrations and a predominant dilution $c-q$ pattern (e.g. UK24) and low TRP concentrations, high
271 rainfall and a predominant concentration $c-q$ pattern (e.g. NO5). The second canonical axis
272 discriminated between flashy, clay catchments with low NO₃-N concentrations, chemostatic NO₃-N and
273 SS $c-q$ response and well-drained, groundwater-dominated catchments with high positive $c-q$ slopes for
274 SS and negative $c-q$ slopes for NO₃-N (Figure 7). These results indicate that TRP and NO₃-N saturation
275 effects, catchment soil type and flashiness provide a good explanation of the observed differences in
276 the $c-q$ slopes between the catchments and determinands.

277 *Robustness of the $c-q$ relationship*

278 To test the robustness of the $c-q$ relationship we compared the slopes for high- and low-frequency
279 datasets, different sampling strategies and nonlinear and non-stationary $c-q$ relationships - in general
280 there were no significant differences. There were no statistically significant differences in the $c-q$ slopes
281 calculated independently from the high- (HF1 and HF2) and low-frequency (LF1 and LF2) datasets

282 (Table ST1) despite much longer coverage of the low-frequency time series (HF1 2009-2015, LF1
283 1990-2015, HF2 2016-2017, LF2 1988-2016). There were no statistically significant differences
284 between c - q slopes for different sampling strategies: time- and flow-proportional sampling for the
285 Swedish catchments (Table ST1 and Figure SF4), despite both datasets only partially overlapping, e.g.
286 for SE1 time-proportional (grab) 1992-2010 and flow-proportional 2004-2017. There was a strong
287 linear relationship between the c - q slopes calculated from both datasets ($R^2=0.88$, $p<0.05$) and the data
288 were generally grouped by the determinand (Figure SF4a) rather than the catchment (Figure SF4b).

289 We examined all datasets for the presence of nonlinear c - q relationships (as $\text{NO}_3\text{-N}_{\text{HF2}}$ and DOC_{HF2} in
290 Figure 1), visually determined the inflection point and fitted two separate linear slopes for low (\leq
291 inflection point discharge) and high (\geq inflection point discharge) flows. Majority of the c - q
292 relationships (92%) showed single linear slopes with the exception of the datasets listed in Table ST8
293 that showed changes in the c - q slope at a given threshold value of flow. The differences between single
294 and dual slopes were significant for TP and SS but not for RP, $\text{NO}_3\text{-N}$, DOC or COND (Table ST8).
295 The threshold value of flow discharge in nonlinear c - q relationships varied between determinands and
296 catchments but in general low flows showed lower c - q slopes than high flows. Both TP and RP showed
297 dilution pattern for low flows and strong concentration pattern for high flows, whereas SS slopes shifted
298 from a moderate to strong concentration pattern (Figure 8). The single c - q slope reflected the dominant
299 c - q relationship for TRP and SS and was the mean value of individual slopes for TP.

300 The c - q relationship can also be affected by non-stationarity in either c or q data e.g. due to the presence
301 of a linear trend in the long-term time series. To test this effect, we calculated linear trends for all high-
302 and low-frequency datasets (Table ST9) and expressed the slopes as an annual percentage trend (Figure
303 9). The mean annual trend varied from -2.2% for TRP to 0.4% for Q and TP and showed the largest
304 variation between the catchments for SS (8.5% SE2^{fp} and -17.9% NO4^{fp}), TRP (16.7% SE7^{fp} and -
305 16.8% UK5) and TP (10.5% SE7^{fp} and -7.0% UK23). The high-frequency datasets showed higher
306 annual trends (e.g. Q HF1 -9.7% and HF2 8.3%) likely due to a shorter length of the time series
307 compared to the low-frequency, long-term datasets. To show the effect of significant linear trends with
308 more than 5% annual change on the c - q slopes, the datasets were split in half and the c - q slopes were

309 calculated independently for each half (Figure SF5). There were no statistically significant differences
310 between the c - q slopes for TP, TRP and SS but the effect varied between the datasets and determinands
311 (Figure SF5). An example (Figure SF6) shows two time series with similar annual trends (-8.4% and -
312 7.8%) TRP (UK6) and NO₃-N (NO₄^{fp}), however the slopes were different only for TRP as indicated by
313 the dilution pattern ($b=-0.16$) in the first half and minor concentration pattern ($b=0.09$) in the second
314 half of the time series. For NO₃-N in the catchment NO₄, similar slopes were observed potentially due
315 to NO₃-N saturation and consistent chemostatic response over time.

316 **Discussion**

317 *c-q slope variation between determinands and catchments*

318 Recent studies highlight that catchment size and dominant land use can be predictors of the variation in
319 concentrations (Abbott et al., 2018; Musolff et al., 2015) and the c - q relationship (Moatar et al., 2017).
320 They show that the variation in the concentrations and nutrient retention declines with the catchment
321 area for both solutes and particulates (Abbott et al., 2018; Cheng and Basu, 2017) and can lead to
322 universal homogenization of the hydrochemical responses downstream in the river network (Basu et
323 al., 2011; Creed et al., 2015). Adding to this homogenization, are the legacy stores of P and N in
324 agricultural soils and unsaturated zone controlling water quality in the long-term for both small (Ascott
325 et al., 2016; Bieroza et al., 2014; Dupas et al., 2016) and large catchments (Howden et al., 2010; Van
326 Meter et al., 2017). A recent study (Bieroza and Heathwaite, 2015) showed that a low-order agricultural
327 stream is a position in the stream network where both the hydrological and biogeochemical processes
328 operate jointly to control the c - q relationship leading to a dynamic equilibrium between the chemostatic
329 and chemodynamic responses.

330 This ongoing research, focusing on large (catchment size and land use) or small scale (storm flow and
331 meteorological controls) controls of the c - q relationship, suggest that headwater catchments (<3rd
332 Strahler order) are critical landscape positions where most of the stream flow and hydrochemical
333 signature of the stream network is generated. These headwater catchments are also the basic landscape
334 units of water quality management and critical areas for combating eutrophication and hypoxia through

335 agri-environmental mitigation measures (Ockenden et al., 2017). Our study adds new evidence to this
336 ongoing work by analysing the variability in the c - q relationships for a range of determinands and small,
337 low-order agricultural catchments.

338 Our results (Figure 6) indicate homogenization of the c - q responses in intensively managed agricultural
339 catchments with many determinands showing typical chemostatic behaviour – a small range of
340 concentrations compared to flow variation. This indicates that despite a large catchment-to-catchment
341 variation in the c - q relationship, the net effect of agricultural management in headwater catchments on
342 stream chemistry is chemostatic. This averaging potentially results from two reasons. Firstly, solutes
343 (DOC, COND and NO₃-N) surprisingly show a very narrow range of c - q slopes for catchments that
344 vary significantly in terms of bedrock, soil type, climate and hydrology. A tendency towards
345 chemostatic c - q relationship in the intensively managed catchments can be a result of agricultural land
346 use overriding the structural differences between catchments (soil, vegetation and topography) and
347 homogenization of hydrological responses (Basu et al., 2011). The long-term agricultural land use leads
348 to shortening of the flow pathways and residence time that will in turn affect many hydrological and
349 biogeochemical processes. Secondly, a large variation in the c - q slopes including both positive and
350 negative values observed between the catchments and determinands can lead to apparent averaging of
351 the c - q responses downstream the river network. This synchrony at the catchment level has been show
352 recently by Abbott et al. (2018) for two nested agricultural catchments. Our results confirm similar
353 effects for a large number of catchments with agricultural land use, varying in geology, climate and
354 soils. On the determinand level, the averaging effect can be exemplified by the c - q responses of RP
355 (dilution pattern) and SS (concentration pattern). These opposing effects result in the near-chemostatic
356 responses for the TP, when the contribution of particulate and soluble fractions of P is similar. Also,
357 some determinands and catchments show dual slopes for low and high flows with the opposing effect
358 on the c - q slopes e.g. dilution at low flows and concentration at high flows for TRP, leading to an overall
359 chemostatic c - q effect.

360 The general strong affinity towards certain c - q behaviour, also shown by Moatar et al. (2017) in the >50
361 km² catchments, was not observed for TRP and NO₃-N c - q responses. For the catchments analysed in

362 our study, subjected to diffuse pollution with no major point sources, with high concentrations the
363 typical response is dilution for TRP and chemostasis for NO₃-N, whereas a concentration pattern is
364 observed for the catchments with lower concentrations (Figure 7). This links to the presence of the P
365 and N legacy stores in agricultural catchments due to excess fertilisation over a long time. The effect of
366 P and N saturation in agricultural catchments on the *c-q* relationship depends on the geology, soil type
367 and the flashiness. In permeable catchments with deep unsaturated zone and low flashiness, excess
368 NO₃-N will gradually accumulate in the subsurface (Ascott et al., 2016; Howden et al., 2010; Van Meter
369 et al., 2017) and produce a chemostatic *c-q* response in the stream (Bieroza et al., 2014). In poorly-
370 drained clay catchments, due to shorter residence times in the subsurface excess NO₃-N will be flushed
371 on a storm-to-storm basis leading to a concentration *c-q* response in the stream, as in HF2. The TRP
372 behaviour is more complex due to its transport duality – it can be transported both as a solute along the
373 subsurface flow pathways (Mellander et al., 2015) and sorbed to particulates and transported along the
374 surface flow pathways (Dupas et al., 2015). A concentration *c-q* pattern is typical for P derived from
375 diffuse agricultural sources but the presence of small rural point sources leads to a dilution pattern at
376 low flows (Withers et al., 2012). When both types of P sources are present, the *c-q* relationship is
377 nonlinear (Figure 8). The transient TRP storage (in bed sediments (Jarvie et al., 2005) or in the riparian
378 zone (Dupas et al., 2015) can also lead to nonlinear *c-q* relationship by introducing delays in stream
379 delivery and hysteretic *c-q* relationships (Bieroza and Heathwaite, 2015; Hoagland et al., 2017).

380 A growing body of research suggests that the *c-q* slope expresses the relative importance between
381 hydrological and biogeochemical controls (Basu et al., 2011; Thompson et al., 2011). Recent analysis
382 of storm events showed that the chemostatic *c-q* responses indicated the dominance of hydrological
383 controls and the chemodynamic *c-q* responses indicated the dominance of biogeochemical controls
384 (Bieroza and Heathwaite, 2015). The *c-q* slope encapsulates both the individual effects of
385 biogeochemical and hydrological process and their synergistic effects and thus represents the
386 catchment's tendency to store and transport solutes and particulates. However, these processes are non-
387 stationary and future land management and climate change will modify their relative balance (Basu et
388 al., 2011). This combined effect on water quality can be difficult to predict due to positive and negative

389 feedbacks between the effect of land management and climate change (Ockenden et al., 2017). We
390 suggest that the c - q slope can be a good measure of catchment's response and resilience to future
391 change. Future land management is likely to reduce P and N concentrations in agricultural catchments,
392 alleviate the effects of P and N saturation and thus reduce the legacy effects on water quality while
393 increased rainfall can increase the flashiness of the catchments, also due to higher seasonal gradients in
394 flow conditions (Ockenden et al., 2017). Our results (Figure 7) suggest that this potential future change
395 scenario (lower NO₃-N and TRP concentrations, higher rainfall and flashiness) will shift the c - q
396 responses in agricultural catchments from chemostatic to chemodynamic (concentration). Apart from
397 being an indicator of these changes, higher c - q slopes will also mean a more dynamic c - q relationship
398 and a higher uncertainty in water quality parameters.

399 *Errors in water quality parameters as a function of the c - q slopes*

400 Previous work focused on the advantages and limitations of the high-frequency *in situ* monitoring in
401 comparison with the traditional low-frequency grab sampling (Bieroza et al., 2014; Cassidy and Jordan,
402 2011; Dupas et al., 2016; Floury et al., 2017). These studies showed how the gain in number of
403 observations due to high-frequency monitoring leads to improved load estimation compared to both
404 actual and re-sampled low-frequency time series, specifically for the flashy catchments and P and SS
405 concentrations (Cassidy and Jordan, 2011; Jordan and Cassidy, 2011; Rozemeijer et al., 2010). The load
406 estimation errors were also compared for determinands showing different stream transport mechanisms
407 – the chemodynamic c - q responses for P and chemostatic for NO₃-N (Bieroza et al., 2014). The authors
408 concluded that the chemostatic c - q pattern resulted in much lower load estimation errors compared to
409 chemodynamic pattern for P and was driven by the groundwater legacy store of NO₃-N. Here, we build
410 on this work and show the errors not only for loads but also for other parameters used in water quality
411 management: c - q slope, mean concentration used as an indicator of the water quality status e.g. for P in
412 the Water Framework Directive (Wade et al., 2012), the 95th percentile used to select water bodies at a
413 risk of pollution e.g. to designate Nitrate Vulnerable Zones.

414 Similarly to previous studies, we showed that errors increase with decreasing sampling frequency, are
415 higher for particulates than solutes and are higher for determinands exhibiting chemodynamic $c-q$
416 behaviour, specifically the concentration pattern. The range of errors observed in our study
417 corresponded well with previous studies (Bieroza et al., 2014; Cassidy and Jordan, 2011), however by
418 not constraining the sampling to typical sampling regimes (e.g. from 9 to 5), we were able to estimate
419 the maximum possible errors. One of the main findings was that underestimation of parameters derived
420 from low-frequency sampling was more severe than overestimation. Most determinands and parameters
421 showed a maximum of one order of magnitude overestimations while the underestimations could reach
422 three orders of magnitude. This could be a serious limitation of the low-frequency sampling for
423 determinands showing highly dynamic flow responses e.g. SS and for flashy catchments with clay soils.
424 For these determinands and catchments, there is a critical need to conduct high-frequency water quality
425 measurements, particularly if those locations are also at high risk of failing to achieve good ecological
426 status. Another limitation could be the estimation of the 95th percentile from the low-frequency NO₃-N
427 sampling for the catchments showing chemodynamic $c-q$ responses e.g. HF2. In this case the potential
428 underestimation of the 95th percentile is up to two orders of magnitude (Table ST5) and could lead to
429 not designating the catchment as a Nitrate Vulnerable Zone.

430 The errors in the $c-q$ slopes followed the same pattern as for the other parameters, low errors for
431 chemostatic and high errors for chemodynamic $c-q$ slopes. However, the $c-q$ slope errors reduced the
432 strength of the effect (e.g. from strong concentration to weak concentration effect) rather than
433 completely changed it (e.g. from the concentration to dilution). The uncertainty in the $c-q$ slopes was
434 also reduced for longer time series. This means that for most of the available long-term water quality
435 time series, the $c-q$ slope should adequately capture the catchment's dominant behaviour in storing and
436 transporting chemicals. The $c-q$ pattern for a given determinand persists even if the sampling changes
437 (e.g. from time- to flow-proportional) or the concentrations show a linear trend. Both cases should
438 however always be checked for potential errors due to differences between flow-proportional and grab
439 sample concentrations or averaging concentration and dilution patterns over time or for different flows
440 in time series exhibiting temporal trends.

441 As our results show, the simple correlation between c - q slope and potential parameter estimation error
442 (Figure 3) should be analysed with caution. Determinands delivered from a number of different sources
443 or during different periods can exhibit different c - q patterns, therefore a good understanding of the main
444 delivery pathways and times when they are active is needed to understand when the errors are likely to
445 be high. Also, for the same determinand and the value of the c - q slope the errors can be enhanced by
446 catchment properties (Figure 3 TURB_{HF2}) e.g. by the presence of fast delivery pathways as in the tile
447 drained clay catchments. For example, NO₃-N showed highly chemostatic behaviour for HF1 likely due
448 to nitrate saturation in the unsaturated zone but a step change from chemostatic to chemodynamic
449 behaviour for HF2. For the clay catchment HF2, due to higher erosion risk, the load estimation errors
450 for TURB were much higher compared with the similar c - q slope for HF1. In special cases, when it is
451 evident from the visual inspection of the data that two different c - q relationships exist for different
452 flows, fitting separate linear regressions is needed. However, for many headwater catchments, the long-
453 term low-frequency datasets have too few samples to calculate statistically significant c - q slopes for
454 different flows, in contrast to high order streams and rivers (Moatar et al., 2017) where 2/3 of cases
455 showed dual slopes (in our study less than 8%). We found that single slopes capture well the dominant
456 c - q relationship for cases where samples were collected at all flows. If there is a bias in the sampling
457 e.g. towards low flows, measurements at high flows are needed to adequately represent the c - q
458 relationship, dominant sources and delivery pathways. This can be achieved either by targeting storms
459 with conventional sampling or by deploying *in situ* optical sensors (Bierozza et al., 2014).

460 *c*- q slope as a robust water quality management tool

461 Our study shows that the c - q slope is a robust descriptor of the catchment's tendency to store and
462 transport chemicals, since similar slopes were observed for both HF and LF datasets and different
463 sampling strategies (time- vs flow-proportional). It can provide a rapid indication of the catchment's
464 status and resilience towards a given chemical – if the chemical exhibits the chemostatic or negative c -
465 q slopes the catchment is likely to be saturated with that chemical, whereas if the chemical shows the
466 concentration pattern its delivery is likely to be transport-limited. In the latter case, appropriate
467 mitigation measures to intercept dominant delivery pathways and target critical source areas could help

468 to reduce pollution. In the case of chemostatic solute behaviour, individual measures and short-term
469 solutions can be ineffective, as is often the case for the catchments failing to meet good water quality
470 status (Harris and Heathwaite, 2012). For these catchments, both long-term and large-scale mitigation
471 approaches are needed (Ockenden et al., 2017; Van Meter et al., 2017) that will require a good
472 cooperation between decision makers, farmers and scientists.

473 Many water quality monitoring programmes are facing financial cuts that will inevitably result in the
474 reduction of the sampling network. Water managers are therefore faced with critical questions: which
475 sampling locations to keep, which long-term time series to continue and how to optimise the sampling
476 to the local conditions. The $c-q$ slope could help address many of these challenges. The optimal
477 sampling frequency required to capture the full range of particulate and solute behaviour depends on
478 their $c-q$ slopes. For chemicals with a chemostatic $c-q$ pattern (e.g. $\text{NO}_3\text{-N}$ and COND), low-frequency
479 sampling (weekly to monthly) for all flows is sufficient to capture the $c-q$ dynamics and obtain accurate
480 estimates of water quality parameters. For chemicals with a dilution $c-q$ pattern (e.g. TRP), daily to
481 weekly sampling is needed to adequately characterise low flow concentrations and target diffuse
482 sources at high flows. Finally, for chemicals with a concentration $c-q$ pattern (e.g. TURB and SS but
483 also TP and $\text{NO}_3\text{-N}$), it is critical to target individual storm events at hourly time step as there is a large
484 variation in the concentrations depending on distribution of the sources and hydrological connectivity.
485 When selecting the sampling locations which should be retained, a priority should be given to those
486 with a large variation in the $c-q$ responses between determinands as indicative of the heterogeneous
487 sources and delivery pathways, with dual slopes and chemodynamic patterns. The latter locations are
488 more likely to be pivot points to the water quality in the stream network as they can experience large
489 variations in concentrations (up to three orders of magnitude) over short storm flows (Bieroza et al.,
490 2014). Dual $c-q$ slope relationships (e.g. dilution at low flows and concentration at high flows) indicate
491 that different sampling regimes and different mitigation measures need to be considered for different
492 combinations of source and delivery pathways. For any water quality monitoring network, the
493 individual sampling points can be optimised depending on their dominant $c-q$ patterns, in terms of
494 sampling frequency and flow conditions to be targeted.

495 Changes in the $c-q$ slope can also aid the location and subsequent evaluation of land management
496 interventions e.g. in the form of mitigation measures to reduce agricultural losses of P, SS and N. To
497 achieve the best environmental outcomes, the mitigation measures should be placed to intercept the
498 main sources and delivery pathways. This spatial targeting can be achieved with critical source areas
499 and critical pathways mapping (Abbott et al., 2018; Thomas et al., 2016) but also by evaluating the $c-q$
500 slopes as discussed above. Improvements in water quality in catchments with a dilution-concentration
501 P pattern are likely to be more difficult to achieve compared to uniform $c-q$ patterns, and will require
502 targeting both low flow (septic tanks or riparian zone) and high flow (diffuse catchment or in-stream)
503 sources. The evaluation of the effectiveness of these mitigation measures can be achieved using $c-q$
504 slopes both in time (by comparing low and high flows or periods before and after implementation of
505 the measures) and space (by comparing locations upstream and downstream of the measures). This
506 critical evidence obtained with $c-q$ slopes is needed both for water managers to comply with the
507 statutory requirements and the farming community to see that their efforts in building and maintaining
508 mitigation measures bring the desired environmental benefits.

509 **Conclusions**

510 The $c-q$ slope is a single metric that expresses the catchment's dominant tendency for storing and
511 transporting solutes and particulates, is easy to calculate from readily available hydrochemical datasets
512 and can be used to effectively guide water quality management. The $c-q$ slope can be used to understand
513 solute and particulate behaviour across spatial (from stream reaches to stream networks and between
514 catchments) and temporal scales, and by this to extrapolate beyond single catchment process
515 understanding (Abbott et al., 2016). As it encapsulates information about dominant biogeochemical and
516 hydrological controls, the $c-q$ slope is a good measure of current balance and future change in any of
517 the underlying processes, e.g. due to land management including mitigation measures or climate
518 change. Agricultural catchments analysed in our study had no major point sources and showed on
519 average strong chemostatic behaviour for TP and $\text{NO}_3\text{-N}$ due to long-term accumulation of agricultural
520 N and P in unsaturated zone and soils. Future reduction in P and N pollution, increased rainfall and

521 flashiness in agricultural catchments are likely to shift this dominant chemostatic behaviour to
522 chemodynamic, concentration c - q responses to flow. For water managers, this shift will require a more
523 targeted approach to water quality monitoring, both in space and time, since the chemodynamic c - q
524 slopes have higher uncertainty in the diagnostic parameters derived from low-frequency sampling e.g.
525 loads, mean or 95th percentile concentrations. To achieve the best outcomes, water management should
526 focus on catchments and determinands showing chemodynamic and dual slope c - q responses. The c - q
527 slope analysis combined with high-frequency monitoring using optical sensors and analysers can
528 provide an effective toolset to evaluate the effectiveness of management interventions. By focusing on
529 low-order agricultural catchments, we provide a critical understanding of the linkages between
530 hydrochemical functioning and eutrophication risks and translate this knowledge into operational
531 responses.

532 **Acknowledgements**

533 This work was funded by the Marie Skłodowska-Curie Fellowship awarded to M. Bieroza (Project
534 HotPaNTS, 657192, European Commission). The authors would like to also acknowledge the funding
535 from the Natural Environment Research Council (NE/M019837/1 awarded to M. Bieroza and
536 NE/G001707/1 awarded to A.L. Heathwaite) and from the Stiftelsen Lantbruksforskning awarded to
537 M. Bieroza (O-16-23-640). The authors would like to thank Lars Bergström from the Swedish
538 University of Agricultural Sciences, Alwyn Hart and Linda Pope from the Environmental Agency, Neil
539 Mullinger and Paddy Keenan from the Lancaster Environment Centre, Maria Blomberg and Lovisa
540 Sternman-Forsberg from the Swedish Monitoring Programme and Mattias Ryman and Niklas
541 Strömbeck from Luode Co.

542 **References**

- 543 Abbott BW, Baranov V, Mendoza-Lera C, Nikolakopoulou M, Harjung A, Kolbe T, et al. Using multi-
544 tracer inference to move beyond single-catchment ecohydrology. *Earth-Science Reviews* 2016;
545 160: 19-42.
- 546 Abbott BW, Gruau G, Zarnetske JP, Moatar F, Barbe L, Thomas Z, et al. Unexpected spatial stability
547 of water chemistry in headwater stream networks. *Ecol Lett* 2018; 21: 296-308.

548 Ameli AA, Beven K, Erlandsson M, Creed IF, McDonnell JJ, Bishop K. Primary weathering rates,
549 water transit times, and concentration-discharge relations: A theoretical analysis for the critical
550 zone. *Water Resources Research* 2017.

551 Ascott MJ, Wang L, Stuart ME, Ward RS, Hart A. Quantification of nitrate storage in the vadose
552 (unsaturated) zone: a missing component of terrestrial N budgets. *Hydrological Processes* 2016;
553 30: 1903-1915.

554 Basu NB, Thompson SE, Rao PSC. Hydrologic and biogeochemical functioning of intensively managed
555 catchments: A synthesis of top-down analyses. *Water Resources Research* 2011; 47: 1-12.

556 Bechmann M, Deelstra J, Stålnacke P, Eggestad HO, Øygarden L, Pengerud A. Monitoring catchment
557 scale agricultural pollution in Norway: policy instruments, implementation of mitigation
558 methods and trends in nutrient and sediment losses. *Environmental Science & Policy* 2008; 11:
559 102-114.

560 Bieroza MZ, Heathwaite AL. Seasonal variation in phosphorus concentration-discharge hysteresis
561 inferred from high-frequency in situ monitoring. *Journal of Hydrology* 2015; 524: 333-347.

562 Bieroza MZ, Heathwaite AL. Unravelling organic matter and nutrient biogeochemistry in groundwater-
563 fed rivers under baseflow conditions: Uncertainty in in situ high-frequency analysis. *Sci Total
564 Environ* 2016; 572: 1520-1533.

565 Bieroza MZ, Heathwaite AL, Mullinger NJ, Keenan PO. Understanding nutrient biogeochemistry in
566 agricultural catchments: the challenge of appropriate monitoring frequencies. *Environ Sci
567 Process Impacts* 2014; 16: 1676-91.

568 Butturini A, Alvarez M, Bernal S, Vazquez E, Sabater F. Diversity and temporal sequences of forms of
569 DOC and NO₃-discharge responses in an intermittent stream: Predictable or random
570 succession? *Journal of Geophysical Research* 2008; 113.

571 Cassidy R, Jordan P. Limitations of instantaneous water quality sampling in surface-water catchments:
572 Comparison with near-continuous phosphorus time-series data. *Journal of Hydrology* 2011;
573 405: 182-193.

574 Chappell NA, Jones TD, Tych W. Sampling frequency for water quality variables in streams: Systems
575 analysis to quantify minimum monitoring rates. *Water Res* 2017; 123: 49-57.

576 Cheng FY, Basu NB. Biogeochemical hotspots: Role of small water bodies in landscape nutrient
577 processing. *Water Resources Research* 2017.

578 Creed IF, McKnight DM, Pellerin BA, Green MB, Bergamaschi BA, Aiken GR, et al. The river as a
579 chemostat: fresh perspectives on dissolved organic matter flowing down the river continuum.
580 *Canadian Journal of Fisheries and Aquatic Sciences* 2015; 72: 1272-1285.

581 Dupas R, Gascuel-Oudou C, Gilliet N, Grimaldi C, Gruau G. Distinct export dynamics for dissolved
582 and particulate phosphorus reveal independent transport mechanisms in an arable headwater
583 catchment. *Hydrological Processes* 2015; 29: 3162-3178.

584 Dupas R, Jomaa S, Musolff A, Borchardt D, Rode M. Disentangling the influence of hydroclimatic
585 patterns and agricultural management on river nitrate dynamics from sub-hourly to decadal
586 time scales. *Sci Total Environ* 2016; 571: 791-800.

587 Evans C, Davies TD. Causes of concentration/discharge hysteresis and its potential as a tool for analysis
588 of episode hydrochemistry. *Water Resources Research* 1998; 34: 129-137.

589 Flourey P, Gaillardet J, Gayer E, Bouchez J, Tallec G, Ansart P, et al. The potamochemical symphony:
590 new progress in the high-frequency acquisition of stream chemical data. *Hydrology and Earth
591 System Sciences* 2017; 21: 6153-6165.

592 Godsey SE, Kirchner JW, Clow DW. Concentration-discharge relationships reflect chemostatic
593 characteristics of US catchments. *Hydrological Processes* 2009; 23: 1844-1864.

594 Harris GP, Heathwaite AL. Why is achieving good ecological outcomes in rivers so difficult?
595 *Freshwater Biology* 2012; 57: 91-107.

596 Hoagland B, Russo TA, Gu X, Hill L, Kaye J, Forsythe B, et al. Hyporheic zone influences on
597 concentration-discharge relationships in a headwater sandstone stream. *Water Resources
598 Research* 2017.

599 Holm S. A Simple Sequentially Rejective Multiple Test Procedure. *Scandinavian Journal of Statistics*
600 1978; 6: 65-70.

601 Howden NJK, Burt TP, Worrall F, Whelan MJ, Bierzoza M. Nitrate concentrations and fluxes in the
602 River Thames over 140 years (1868-2008): are increases irreversible? *Hydrological Processes*
603 2010; 24: 2657-2662.

604 Jarvie HP, Jürgens MD, Williams RJ, Neal C, Davies JLL, Barrett C, et al. Role of river bed sediments
605 as sources and sinks of phosphorus across two major eutrophic UK river basins: the Hampshire
606 Avon and Herefordshire Wye. *Journal of Hydrology* 2005; 304: 51-74.

607 Jordan P, Cassidy R. Technical Note: Assessing a 24/7 solution for monitoring water quality loads in
608 small river catchments. *Hydrology and Earth System Sciences* 2011; 15: 3093-3100.

609 Jordan P, Melland AR, Mellander PE, Shortle G, Wall D. The seasonality of phosphorus transfers from
610 land to water: implications for trophic impacts and policy evaluation. *Sci Total Environ* 2012;
611 434: 101-9.

612 Jordan P, Menary W, Daly K, Kiely G, Morgan G, Byrne P, et al. Patterns and processes of phosphorus
613 transfer from Irish grassland soils to rivers—integration of laboratory and catchment studies.
614 *Journal of Hydrology* 2005; 304: 20-34.

615 Krause S, Heathwaite L, Binley A, Keenan P. Nitrate concentration changes at the groundwater-surface
616 water interface of a small Cumbrian river. *Hydrological Processes* 2009; 23: 2195-2211.

617 Kyllmar K, Forsberg LS, Andersson S, Mårtensson K. Small agricultural monitoring catchments in
618 Sweden representing environmental impact. *Agriculture, Ecosystems & Environment* 2014;
619 198: 25-35.

620 Lawler DM, Petts GE, Foster ID, Harper S. Turbidity dynamics during spring storm events in an urban
621 headwater river system: the Upper Tame, West Midlands, UK. *Sci Total Environ* 2006; 360:
622 109-26.

623 Legendre L, Legendre P. *Numerical Ecology*. Amsterdam: Elsevier Scientific Pub. Co., 1998.

624 Lloyd CE, Freer JE, Johnes PJ, Collins AL. Using hysteresis analysis of high-resolution water quality
625 monitoring data, including uncertainty, to infer controls on nutrient and sediment transfer in
626 catchments. *Sci Total Environ* 2016; 543: 388-404.

627 Mellander P-E, Jordan P, Shore M, Melland AR, Shortle G. Flow paths and phosphorus transfer
628 pathways in two agricultural streams with contrasting flow controls. *Hydrological Processes*
629 2015; 29: 3504-3518.

630 Moatar F, Abbott BW, Minaudo C, Curie F, Pinay G. Elemental properties, hydrology, and biology
631 interact to shape concentration-discharge curves for carbon, nutrients, sediment, and major
632 ions. *Water Resources Research* 2017.

633 Musolff A, Schmidt C, Selle B, Fleckenstein JH. Catchment controls on solute export. *Advances in*
634 *Water Resources* 2015; 86: 133-146.

635 Ockenden MC, Hollaway MJ, Beven KJ, Collins AL, Evans R, Falloon PD, et al. Major agricultural
636 changes required to mitigate phosphorus losses under climate change. *Nat Commun* 2017; 8:
637 161.

638 Rode M, Wade AJ, Cohen MJ, Hensley RT, Bowes MJ, Kirchner JW, et al. Sensors in the Stream: The
639 High-Frequency Wave of the Present. *Environ Sci Technol* 2016; 50: 10297-10307.

640 Rozemeijer JC, van der Velde Y, van Geer FC, de Rooij GH, Torfs PJJF, Broers HP. Improving Load
641 Estimates for NO₃ and P in Surface Waters by Characterizing the Concentration Response to
642 Rainfall Events. *Environmental Science & Technology* 2010; 44: 6305-6312.

643 Tetzlaff D, Carey SK, McNamara JP, Laudon H, Soulsby C. The essential value of long-term
644 experimental data for hydrology and water management. *Water Resources Research* 2017; 53:
645 2598-2604.

646 Thomas IA, Mellander PE, Murphy PNC, Fenton O, Shine O, Djodjic F, et al. A sub-field scale critical
647 source area index for legacy phosphorus management using high resolution data. *Agriculture,*
648 *Ecosystems & Environment* 2016; 233: 238-252.

649 Thompson SE, Basu NB, Lascrain J, Aubeneau A, Rao PSC. Relative dominance of hydrologic versus
650 biogeochemical factors on solute export across impact gradients. *Water Resources Research*
651 2011; 47: n/a-n/a.

652 Ulén B, Djodjic F, Etana A, Johansson G, Lindström J. The need for an improved risk index for
653 phosphorus losses to water from tile-drained agricultural land. *Journal of Hydrology* 2011; 400:
654 234-243.

655 USDA. Module 3 - USDA Textural Soil Classification. Study Guide. United States Department of
656 Agriculture, Soil Mechanics Level I 1987: 1-53.

657 Wade AJ, Palmer-Felgate EJ, Halliday SJ, Skeffington RA, Loewenthal M, Jarvie HP, et al.
658 Hydrochemical processes in lowland rivers: insights from in situ, high-resolution monitoring.
659 Hydrology and Earth System Sciences 2012; 16: 4323-4342.

660 Van Meter KJ, Basu NB, Van Cappellen P. Two centuries of nitrogen dynamics: Legacy sources and
661 sinks in the Mississippi and Susquehanna River Basins. Global Biogeochemical Cycles 2017;
662 31: 2-23.

663 Withers PJA, May L, Jarvie HP, Jordan P, Doody D, Foy RH, et al. Nutrient emissions to water from
664 septic tank systems in rural catchments: Uncertainties and implications for policy.
665 Environmental Science & Policy 2012; 24: 71-82.

666

Table 1 Study catchment characteristics including permeability (high H, moderate M and low L), soil texture, Strahler order, mean rainfall and runoff flashiness (Jordan et al., 2005). Agricultural land use comprises arable, horticulture and grassland land uses. Soil texture: clay (C), clay loam (CL), silt loam (SiL), loam (L), sandy loam (SaL), sand (Sa), silt (Si), loamy sand (LSa), silty clay (SiC) (USDA, 1987). UK soil data were obtained from the UK Soil Observatory Map Viewer (<http://www.ukso.org/home.html>), and flow data from the National River Flow Archive (<https://nrfa.ceh.ac.uk/>). Catchment codes: HF – high-frequency dataset, LF – low-frequency dataset, SE1-10 Swedish catchments, NO1-10 Norwegian catchments and UK1-42 UK catchments. Water quality monitoring starting year is also given

Catchment	Area (km ²)	Longitude, latitude	Permeability	Soil texture	Agricultural land use (%)	Strahler order	Rainfall (mm)	Flashiness (Q5:Q95)	Water quality monitoring from
HF1 (LF1)	54.0	-2.6, 54.5	M	CL, SiL	85	3	957 [^]	74	2009/1990
HF2 (LF2)	7.4	16.1, 58.3	L	C	54	2	594 [*]	237	2017/1988
SE1	33.0	17.1, 59.6	M	CL	59	2	623 [*]	605	1992
SE2	16.3	14.9, 58.5	H	SaL	89	2	506 [*]	279	1988
SE3	7.4	16.1, 58.3	L	C	54	2	594 [*]	237	1988
SE4	1.8	13.4, 57.2	H	LSa	70	2	1066 [*]	103	1993
SE5	4.7	18.5, 57.7	H	SaL	84	2	587 [*]	372	1989
SE6	7.8	12.9, 56.2	M	C, SaL	86	2	719 [*]	330	1988
SE7	8.3	13.2, 55.4	H	SaL, L	93	2	709 [*]	556	1992
SE8	13.9	13.3, 56.7	M	SaL, SiL	85	2	886 [*]	17	1996
SE9	7.6	12.7, 58.4	L	C	92	2	655 [*]	214	1988
SE10	5.7	16.1, 59.2	L	C	56	2	539 [*]	605	1993
NO1	4.5	10.8, 59.6	H	LSa	61	2	785 ^x	38	1993
NO2	6.8	11.3, 60.1	L	SiC	65	3	665	42	1990
NO3	3.1	10.7, 60.8	L	C	68	2	585 ^x	17	1985
NO4	1.7	10.7, 59.3	L	CL	62	1	829 ^x	10	2004
NO5	0.9	8.4, 58.3	H	Sa	48	2	1230 ^x	8	1991
NO6	19.4	8.7, 60.6	L	SiC	80	3	892 ^x	79	1992
NO7	29.3	5.7, 59.9	L	C	85	2	1180 ^x	20	1995
NO8	1.0	5.6, 58.7	H	LSa	88	1	1180 ^x	7	1985
NO9	1.5	14.7, 67.2	H	Sa	35	2	1020 ^x	19	1994
NO10	1.7	9.0, 61.1	H	LSa	41	1	575 ^x	11	1991
UK1	9.0	-0.3, 55.2	M	CL	86	2	669 [*]	80	2000
UK2	57.2	-0.3, 54.0	H	L	95	3	699 [*]	12	2000
UK3	41.9	-0.7, 53.8	H	SaL	87	2	690 [*]	14	2000
UK4	47.0	-0.9, 53.9	L	CL	86	3	654 [*]	39	2000
UK5	12.9	-0.6, 54.2	M	L	90	2	735 [*]	15	2000
UK6	32.2	-1.2, 53.2	H	SaL	77	2	668 [*]	4	2000
UK7	46.2	-0.1, 53.1	L	CL	86	3	655 [*]	8	2000
UK8	55.2	0.0, 53.4	H	SaL	90	2	699 [*]	9	2000
UK9	54.7	-0.4, 53.4	M	CL	96	3	614 [*]	46	2000
UK10	48.4	-0.4, 53.0	M	L	87	2	601 [*]	168	2000
UK11	50.5	-0.6, 52.9	H	SaL	88	3	656 [*]	12	2000
UK12	51.3	-0.6, 52.8	H	SaL	83	3	642 [*]	41	2010
UK13	20.8	-0.9, 52.5	L	C	90	3	648 [*]	127	2000
UK14	22.3	-0.5, 52.7	M	CL	71	3	616 [*]	19	2000
UK15	58.3	-0.7, 52.4	M	CL	74	3	634 [*]	18	2000
UK16	38.8	-0.6, 51.9	M	SaL	91	4	640 [*]	53	2006
UK17	59.0	0.5, 52.9	H	Sa	90	2	688 [*]	9	2000
UK18	28.3	1.0, 52.5	H	L	89	2	608 [*]	26	2000
UK19	36.4	0.3, 52.2	H	SiL	90	2	565 [*]	7	2000
UK20	47.7	0.5, 52.8	H	Sa	87	2	685 [*]	5	2000

UK21	16.0	0.0, 52.1	H	SiL	70	2	561*	6	2000
UK22	59.8	1.5, 52.8	H	SiL	88	3	589*	65	2007
UK23	49.3	1.4, 52.2	M	SaL	81	2	631*	3	2000
UK24	54.9	0.9, 52.0	M	L	88	3	597*	16	2010
UK25	53.9	0.7, 52.1	M	SiL	90	2	566*	10	2000
UK26	47.4	0.7, 52.0	H	SaL	91	3	589*	30	2000
UK27	58.6	0.5, 52.0	H	SaL	95	3	560*	38	2000
UK28	28.3	0.6, 51.8	H	L	94	3	589*	215	2000
UK29	60.7	0.0, 51.7	L	CL	83	2	572*	6	2000
UK30	38.4	0.2, 51.8	L	C	72	2	616*	88	2000
UK31	54.6	0.2, 51.9	L	CL	83	3	599*	44	2000
UK32	25.9	0.0, 51.9	M	SaL	73	2	609*	24	2013
UK33	50.4	-1.3, 51.4	H	Sa	93	3	625*	36	2000
UK34	49.2	-1.7, 51.4	H	SaL	84	1	716*	8	2000
UK35	59.2	-1.9, 51.7	H	SaL	86	1	769*	129	2000
UK36	18.5	1.3, 51.3	H	SaL	77	2	702*	48	2000
UK37	37.7	-2.1, 51.6	H	SaL	87	1	723*	73	2000
UK38	28.2	-2.3, 52.6	M	CL	89	2	792*	53	2000
UK39	54.9	-2.5, 52.8	M	L	78	3	706*	17	2000
UK40	25.0	-2.2, 52.3	H	Sa	92	2	677*	8	2000
UK41	53.4	-2.4, 52.8	M	SaL	81	2	653*	12	2000
UK42	33.6	-0.4, 51.8	M	SaL	93	3	712*	13	2000

*1961-1990, ^1999-2014, ^1990-2015

Table 2 Resampled water quality datasets (mean number of samples N , mean concentration μ , standard deviation of the concentration δ and maximum value Max) based on 10,000 Monte Carlo iterations

Parameter	Sampling	HF1				HF2			
		N	μ	δ	Max	N	μ	δ	Max
TP (mg l^{-1})	<i>HF</i>	18 364	0.04	0.08	1.63	7 024	0.28	0.12	1.40
	<i>Daily</i>	764	0.04	0.08	0.99	144	0.27	0.11	0.88
	<i>Weekly</i>	110	0.04	0.07	0.60	22	0.28	0.10	0.50
	<i>Fortnightly</i>	55	0.04	0.07	0.42	11	0.28	0.09	0.42
	<i>Monthly</i>	26	0.04	0.06	0.28	6	0.27	0.08	0.34
TRP (mg l^{-1})	<i>HF</i>	32 688	0.04	0.03	0.99	7 024	0.16	0.06	0.34
	<i>Daily</i>	997	0.03	0.03	0.43	144	0.16	0.06	0.33
	<i>Weekly</i>	143	0.03	0.03	0.22	22	0.16	0.06	0.27
	<i>Fortnightly</i>	71	0.03	0.03	0.17	11	0.16	0.06	0.25
	<i>Monthly</i>	33	0.03	0.03	0.13	6	0.15	0.06	0.20
TURB (NTU)	<i>HF</i>	44 893	2.48	4.61	242.20	13 766	35.12	39.70	838.72
	<i>Daily</i>	1 209	2.36	4.89	94.30	185	34.75	38.14	314.57
	<i>Weekly</i>	175	2.40	4.53	46.92	27	36.78	34.88	154.09
	<i>Fortnightly</i>	87	2.38	4.19	33.15	14	35.65	32.37	113.07
	<i>Monthly</i>	42	2.37	3.67	21.58	7	34.88	28.96	78.55
NO $_3$ -N (mg l^{-1})	<i>HF</i>	36 779	2.33	0.47	7.46	13 763	3.14	3.27	11.91
	<i>Daily</i>	799	2.45	0.47	4.60	185	3.14	3.27	10.20
	<i>Weekly</i>	115	2.46	0.47	3.75	27	3.29	3.07	9.87
	<i>Fortnightly</i>	58	2.46	0.47	3.56	14	3.19	3.04	9.39
	<i>Monthly</i>	27	2.46	0.46	3.38	7	3.12	2.93	6.99
COND/DOC (μ Sm $^{-1}$ /mg l^{-1})	<i>HF</i>	42 890	425.03	69.50	1291.00	13 766	27.61	11.09	71.78
	<i>Daily</i>	1 158	434.59	64.62	1042.65	185	27.53	11.06	61.72
	<i>Weekly</i>	167	434.54	63.92	702.34	27	28.20	11.29	52.05
	<i>Fortnightly</i>	83	434.68	63.22	623.59	14	27.46	11.09	47.71
	<i>Monthly</i>	40	435.30	61.75	565.75	7	27.49	11.40	42.99

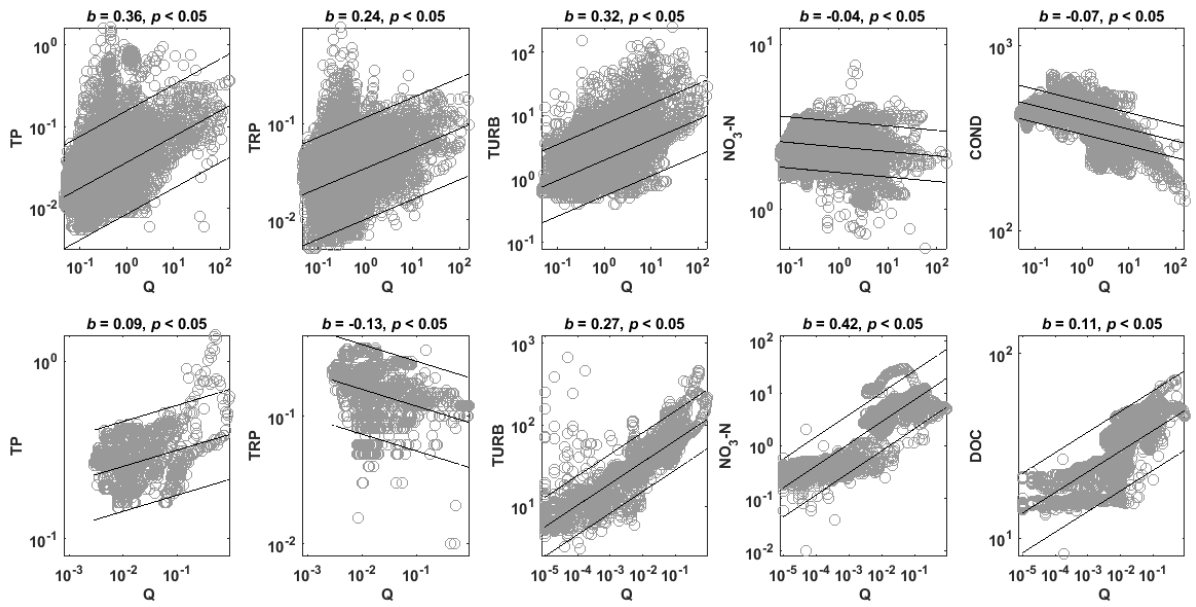


Figure 1 Concentration-discharge (c - q) relationship for the two high-frequency datasets (**HF1** top row and **HF2** bottom row) including the following determinands TP, TRP, TURB, NO₃-N and COND/DOC (columns). Slope of the c - q relationship b is given along with the p value. Both axes are in logarithmic scale

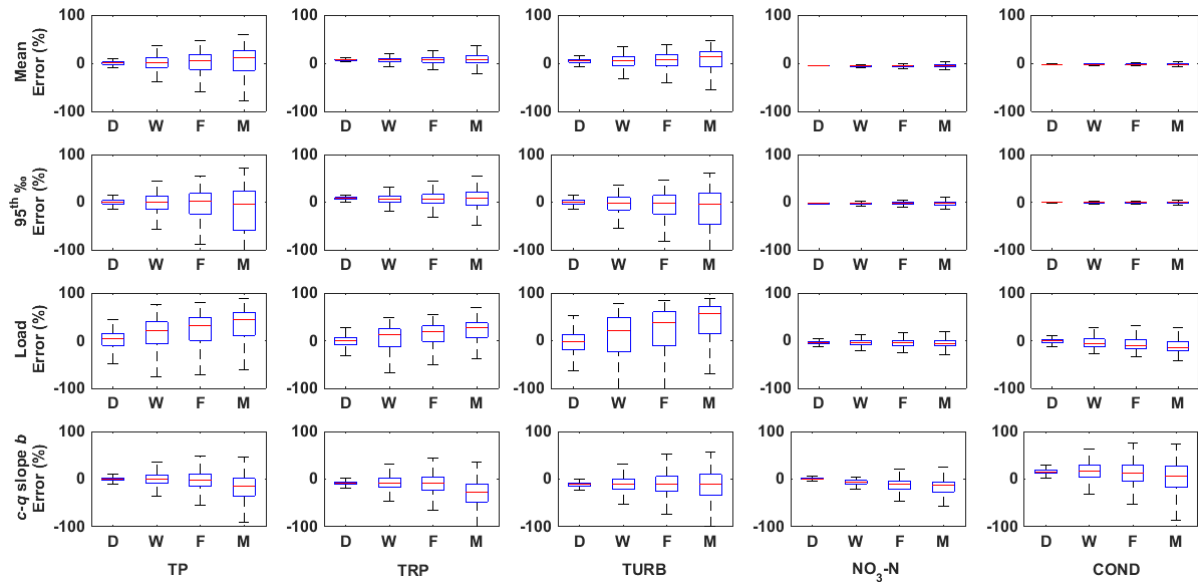


Figure 2 Relative errors in mean (top row), 95th percentile (second row), load estimation (third row) and c - q slope b (bottom row) for **HF1** for TP, TRP, TURB, NO₃-N and COND. The central red mark is the median, the edges of the box are the 25th and 75th percentiles, the black whiskers extend to the most extreme data points. For better clarity the figure does not contain outliers (given in Supplementary Figure SF1)

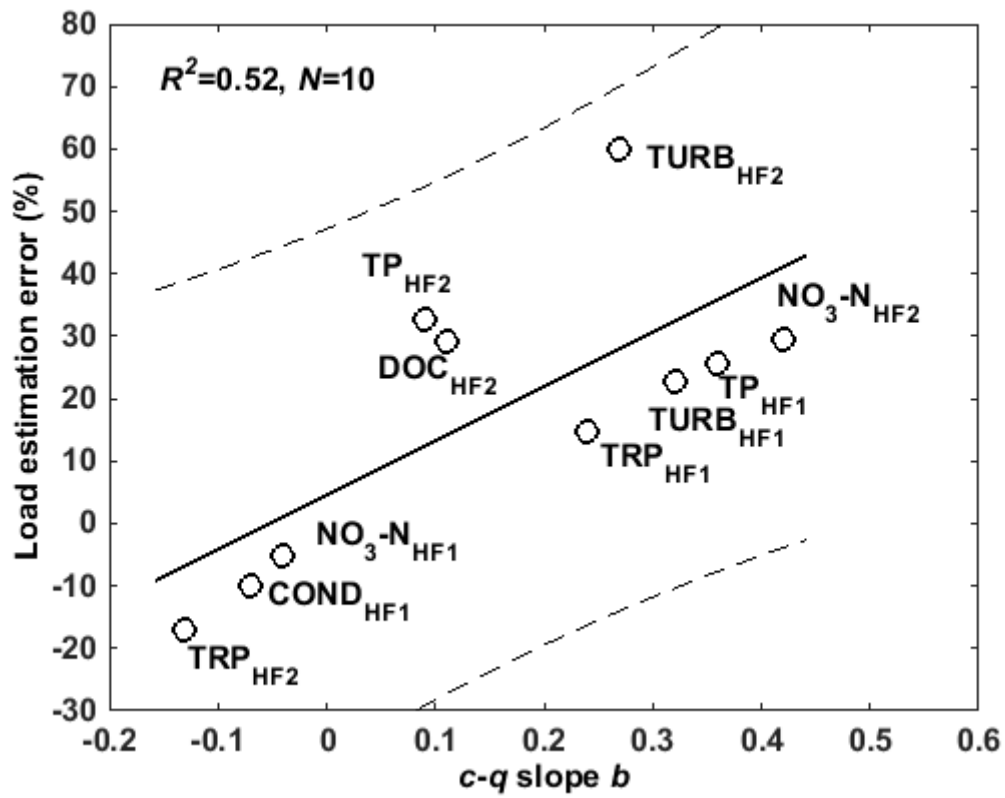


Figure 3 Relationship between c - q slope b and mean relative error in load estimation based on the 10,000 Monte Carlo simulation for all determinands in HF1 and HF2

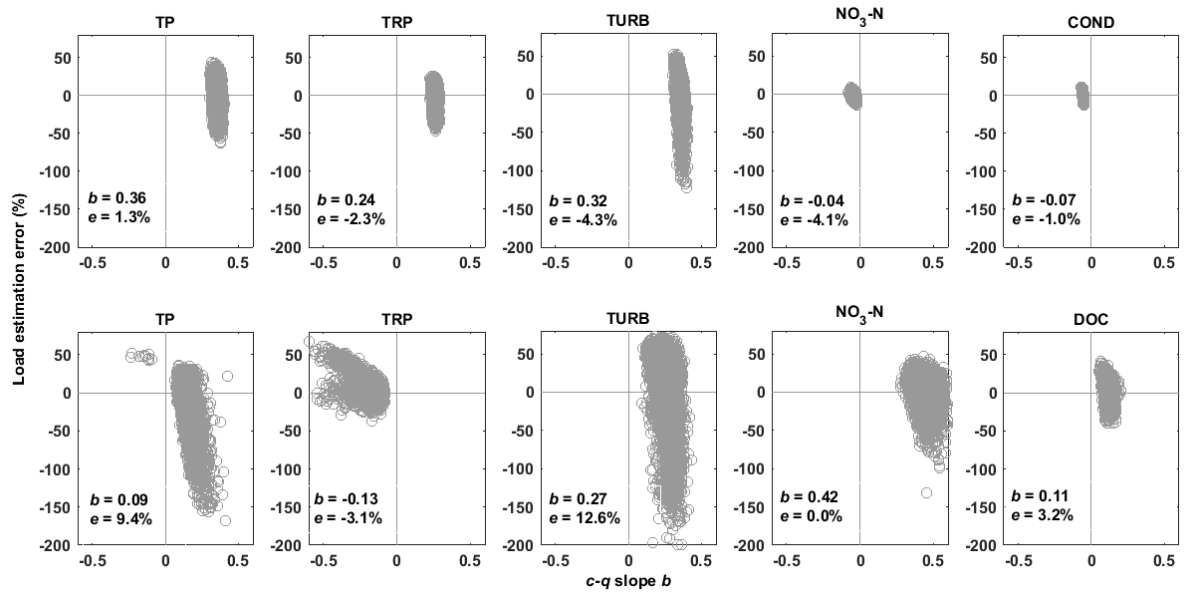


Figure 4 Daily load estimation errors (%) vs. *c-q* slope b based on 10,000 Monte Carlo simulations for two high-frequency datasets (HF1 top row and HF2 bottom row). Mean slope b and load estimation error e are given

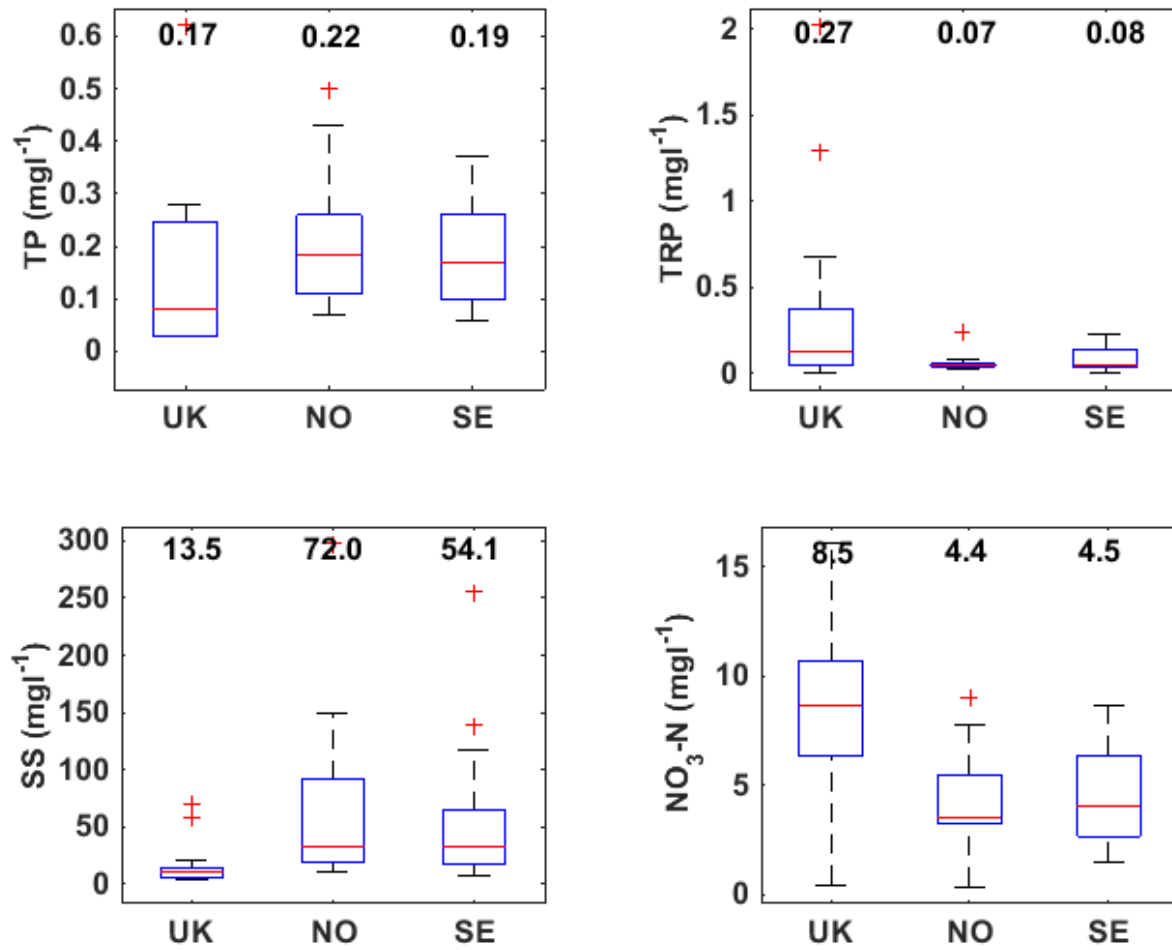


Figure 5 Analysis of variance (Kruskal-Wallis one-way ANOVA) for the mean TP, TRP, SS and NO₃-N concentrations per catchments' location (UK, Norway NO and Sweden SE). The central red mark is the median, the edges of the box are the 25th and 75th percentiles, the black whiskers extend to the most extreme data points and outliers are plotted as red crosses. Mean values are given as numbers

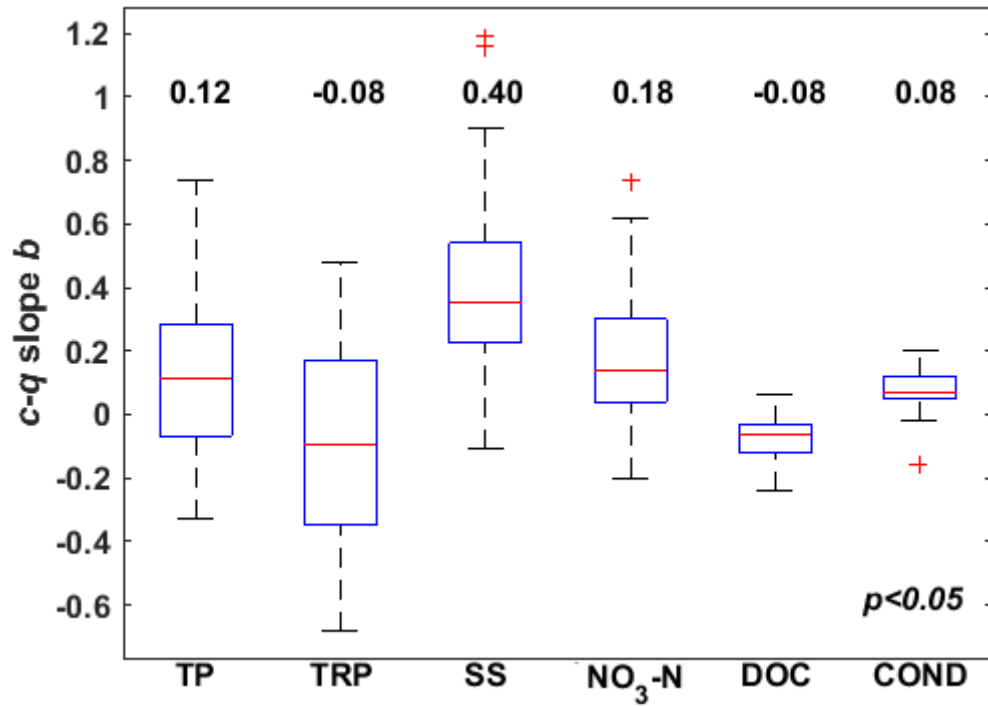


Figure 6 Analysis of variance (Kruskal-Wallis one-way ANOVA) for the c - q slopes per determinand ($N=76$). The central red mark is the median, the edges of the box are the 25th and 75th percentiles, the black whiskers extend to the most extreme data points and outliers are plotted as red crosses. Mean values are given as numbers above boxplots

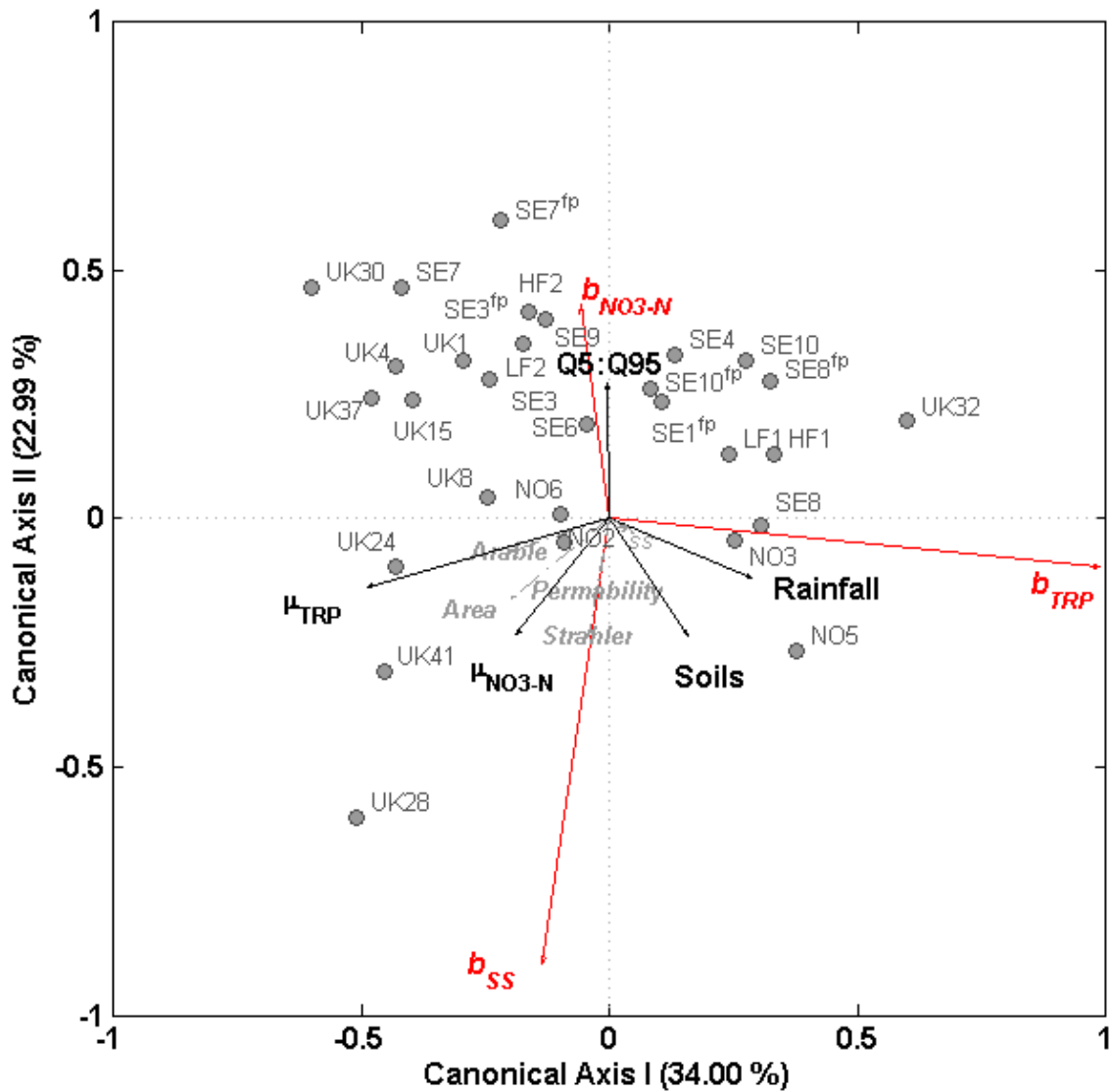


Figure 7 The redundancy analysis distance biplot showing ordination of selected explanatory (Area – catchment area, Arable – agricultural land use percentage, Permeability – 1 low, 2 moderate and 3 high, Q5:Q95 - the flashiness index, Soils - soil texture 1 clay soils, 2 loam soils and 3 sand soils, Strahler order; Table 1) and response variables (c - q slopes b_{TRP} , b_{SS} and b_{NO3-N}). The length of explanatory vectors indicates strength of the relationship with the scores of canonical axes. Distances among individual catchments (grey dots) are approximations of their Euclidean distances. Projecting a catchment at the right angle onto the response vector approximates a value of the c - q slope for that determinand. The angles between response and explanatory vectors indicate their correlation (Legendre and Legendre, 1998)

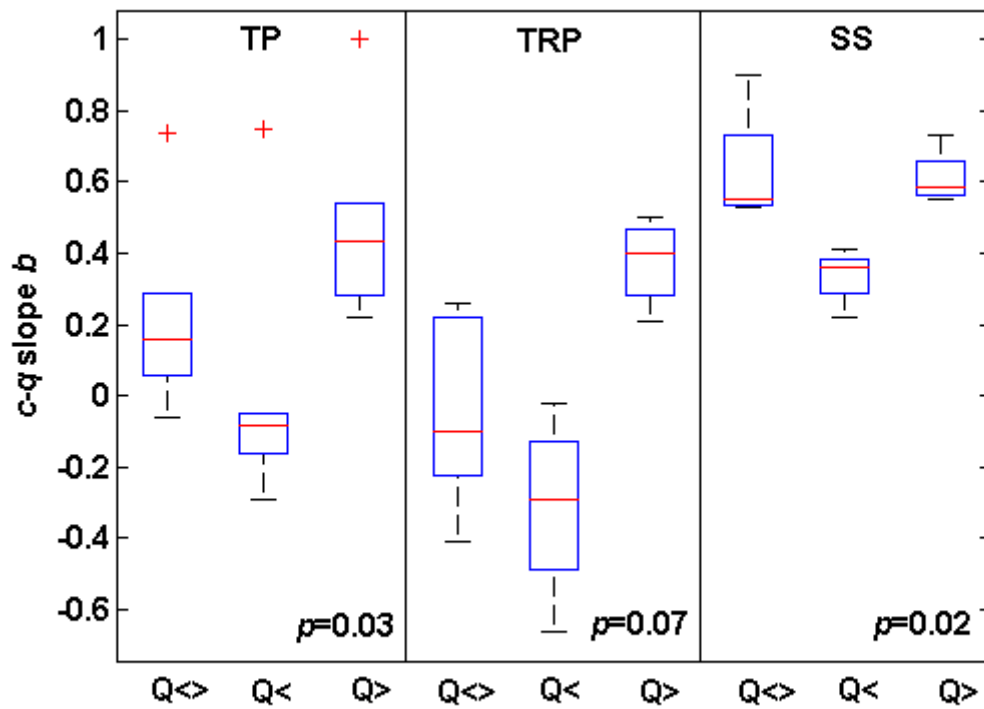


Figure 8 Analysis of variance (Kruskal-Wallis one-way ANOVA) for the c - q relationships showing step changes ($N=6$) in slope values: single linear slope ($Q<>$) and two linear c - q slopes ($Q<$ for flows lower than the threshold value Q and $Q>$ for flows higher than the threshold value Q). The data are also shown in Supplementary Table ST8. The central red mark is the median, the edges of the box are the 25th and 75th percentiles, the black whiskers extend to the most extreme data points and outliers are plotted as red crosses

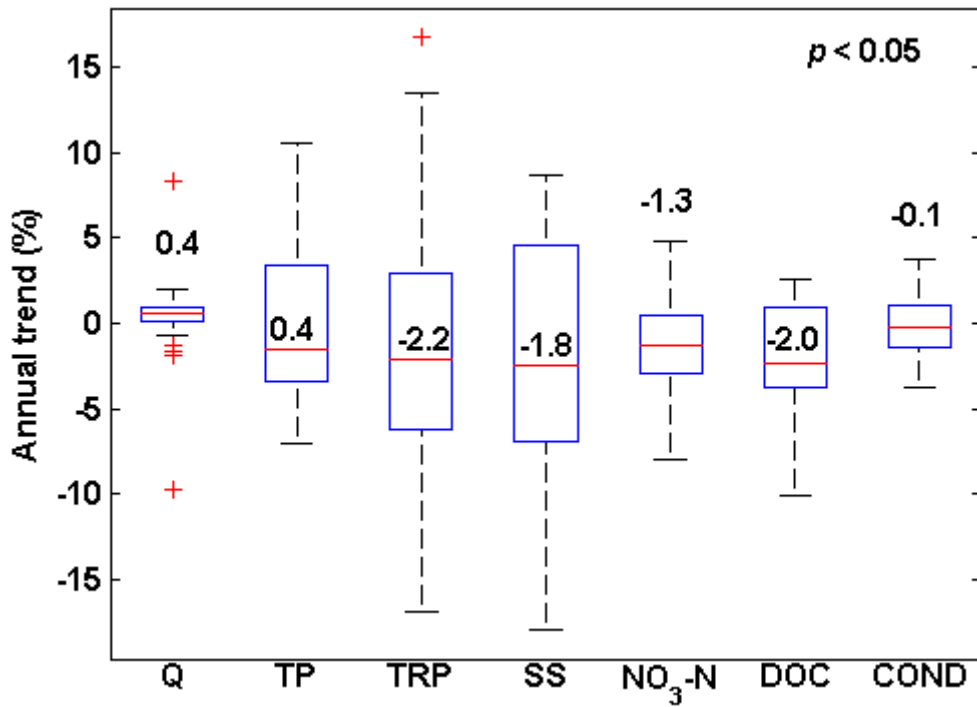


Figure 9 Analysis of variance (Kruskal-Wallis one-way ANOVA) for the annual linear trends per determinand for the flow and water quality datasets ($N=76$). The data are also shown in Supplementary Table ST9. The central red mark is the median, the edges of the box are the 25th and 75th percentiles, the black whiskers extend to the most extreme data points and outliers are plotted as red crosses. Mean values are given as numbers

NO2^{fp}	395	0.50	0.49	0.27	396	0.06	0.06	-0.09	396	297.4	413.4	0.54	396	3.46	1.90	-0.08	-	-	-	-
NO3^{fp}	661	0.08	0.13	0.37	654	0.03	0.03	0.21	661	21.00	53.54	0.56	661	7.80	3.53	0.04	-	-	-	-
NO4^{fp}	111	0.43	0.39	-0.13	111	0.24	0.23	-0.22	111	46.32	81.56	-0.03	111	9.03	4.73	0.01	-	-	-	-
NO5^{fp}	450	0.26	0.34	0.74	421	0.05	0.03	0.37	450	52.26	92.91	0.89	448	4.17	2.24	0.23	-	-	-	-
NO6^{fp}	586	0.26	0.27	0.21	204	0.08	0.09	-0.09	583	149.4	260.6	0.54	586	3.48	2.25	0.05	-	-	-	-
NO7^{fp}	542	0.15	0.11	-0.02	207	0.05	0.05	0.12	335	11.18	9.95	0.17	536	3.52	1.17	0.15	-	-	-	-
NO8^{fp}	432	0.16	0.14	0.05	432	0.06	0.05	0.15	432	11.39	17.39	0.00	429	4.75	1.11	-0.07	-	-	-	-
NO9^{fp}	576	0.11	0.09	0.15	576	0.06	0.06	0.14	576	19.53	25.07	0.53	576	0.38	0.28	-0.03	-	-	-	-
NO10^{fp}	501	0.07	0.15	0.26	501	0.03	0.10	0.02	498	20.57	46.21	0.38	501	2.58	1.13	0.12	-	-	-	-
UK1	-	-	-	-	139	0.17	0.11	-0.26	96	12.03	15.51	0.36	141	3.01	2.00	0.38	65	888.9	460.5	-0.03
UK2	22	0.03	0.03	-0.18	173	0.05	0.17	0.27	173	11.17	15.41	0.08	174	10.63	1.27	0.06	123	615.3	108.2	0.00
UK3	-	-	-	-	205	0.07	0.17	0.12	166	11.93	22.69	0.77	209	11.71	2.09	0.10	159	724.3	132.3	-0.03
UK4	-	-	-	-	127	0.13	0.26	-0.41	172	4.70	3.94	0.24	127	9.38	2.06	0.07	42	690.8	96.36	-0.01
UK5	-	-	-	-	50	0.02	0.01	0.04	-	-	-	-	50	9.57	0.91	-0.03	54	665.8	49.59	0.04
UK6	21	0.10	0.02	0.24	210	0.13	0.09	-0.08	129	7.11	3.53	0.00	178	14.44	1.50	0.00	114	1770	429.5	-0.12
UK7	-	-	-	-	89	0.46	0.12	-0.10	5	5.00	2.12	0.32	54	11.27	1.58	-0.03	-	-	-	-
UK8	-	-	-	-	189	0.04	0.02	-0.21	142	9.52	12.18	0.55	152	10.64	1.55	0.13	138	570.8	110.4	0.05
UK9	-	-	-	-	210	0.43	0.35	-0.04	168	18.64	27.97	0.33	139	8.47	2.32	0.04	166	735.5	89.29	-0.01
UK10	-	-	-	-	71	0.68	0.56	-0.36	-	-	-	-	104	13.99	6.71	0.27	49	1088	248.9	-0.07
UK11	206	0.03	0.02	0.09	207	0.02	0.01	0.00	165	5.55	11.62	0.21	184	10.30	2.40	0.27	158	670.7	64.62	-0.03
UK12	-	-	-	-	176	0.36	0.25	-0.42	142	10.19	22.93	0.34	152	12.09	2.97	0.01	126	970.6	184.2	-0.12
UK13	-	-	-	-	164	0.27	0.31	-0.41	-	-	-	-	110	4.37	3.67	0.58	122	764.5	141.9	-0.07
UK14	-	-	-	-	79	0.02	0.01	0.06	-	-	-	-	79	6.95	2.25	0.27	79	731.1	282.9	0.03
UK15	-	-	-	-	140	0.20	0.13	-0.34	64	20.74	51.07	0.44	88	5.48	2.70	0.34	156	758.6	117.3	-0.05
UK16	46	0.21	0.17	0.28	224	0.10	0.08	0.00	-	-	-	-	164	5.71	3.86	0.50	155	782.1	78.08	-0.05
UK17	-	-	-	-	172	0.03	0.01	0.08	167	6.13	8.14	0.06	142	12.48	0.91	0.10	124	751.5	62.50	-0.01
UK18	-	-	-	-	90	0.66	0.46	-0.63	-	-	-	-	63	9.67	2.25	0.07	44	895.3	84.03	-0.01
UK19	-	-	-	-	118	0.38	0.18	-0.38	-	-	-	-	82	14.01	0.66	0.05	93	747.0	29.85	0.06
UK20	-	-	-	-	141	0.03	0.01	0.14	169	7.55	3.87	0.42	178	11.38	0.65	0.07	94	691.2	98.08	0.00
UK21	-	-	-	-	182	2.02	1.70	-0.20	115	19.70	18.07	-0.09	146	16.06	3.37	0.04	131	1332	324.0	-0.14
UK22	217	0.06	0.03	0.53	187	0.03	0.01	0.06	331	6.82	5.13	1.16	151	3.37	0.72	0.40	225	814.2	50.73	-0.05
UK23	927	0.62	1.19	0.29	1015	0.27	0.13	-0.01	926	58.56	144.2	0.90	978	10.83	3.05	0.03	67	1043	122.6	-0.12

UK24	-	-	-	-	169	0.27	0.13	-0.34	168	9.30	11.18	0.73	140	7.93	2.04	0.14	155	817.4	55.76	-0.02
UK25	-	-	-	-	101	0.12	0.12	-0.02	-	-	-	-	65	6.87	4.65	0.41	52	851.0	73.76	-0.06
UK26	-	-	-	-	134	0.07	0.04	0.08	-	-	-	-	98	5.90	3.76	0.37	113	840.7	70.57	-0.04
UK27	-	-	-	-	142	1.30	1.32	-0.68	-	-	-	-	103	10.82	6.20	0.05	100	936.8	188.9	-0.10
UK28	-	-	-	-	188	0.55	0.27	-0.36	141	14.75	35.26	1.19	152	10.61	1.74	-0.11	151	986.9	150.4	-0.22
UK29	-	-	-	-	176	0.51	0.35	-0.38	72	13.40	25.19	0.55	140	7.40	3.96	0.07	82	832.7	194.6	-0.02
UK30	-	-	-	-	138	0.56	0.35	-0.55	123	13.67	13.64	0.18	102	7.10	3.74	0.29	44	819.1	125.4	-0.02
UK31	-	-	-	-	122	0.08	0.16	0.06	6	13.74	5.89	0.62	85	5.63	2.19	0.14	18	734.8	130.8	-0.09
UK32	-	-	-	-	209	0.07	0.05	0.47	168	6.80	15.78	0.29	173	9.94	2.10	0.11	115	743.4	37.60	-0.03
UK33	-	-	-	-	-	-	-	-	-	-	-	-	106	8.70	1.60	0.22	18	668.1	26.04	0.03
UK34	20	0.03	0.01	-0.04	92	0.05	0.05	0.26	20	3.64	0.86	0.04	92	7.94	0.56	0.02	17	606.8	23.77	0.03
UK35	-	-	-	-	114	0.02	0.01	0.00	160	5.19	5.46	-0.03	85	8.87	1.19	0.07	28	543.9	93.23	-0.02
UK36	-	-	-	-	134	0.23	0.33	0.16	-	-	-	-	107	7.22	3.77	0.36	-	-	-	-
UK37	-	-	-	-	167	0.20	0.15	-0.42	159	11.54	18.13	0.40	202	6.52	3.21	0.25	89	777.1	223.3	-0.17
UK38	-	-	-	-	161	0.09	0.10	0.29	175	11.15	12.79	0.69	161	8.55	1.71	-0.02	68	735.9	107.6	-0.11
UK39	-	-	-	-	84	0.09	0.10	-0.02	60	12.58	12.96	0.17	84	7.90	1.93	0.18	80	586.1	53.22	0.02
UK40	-	-	-	-	-	-	-	-	-	-	-	-	104	9.04	1.96	-0.19	48	813.9	149.4	-0.18
UK41	-	-	-	-	144	0.39	0.21	-0.35	6	8.91	8.83	0.88	106	10.15	1.59	-0.05	51	645.4	120.6	-0.21
UK42	-	-	-	-	151	0.01	0.01	0.32	141	3.84	0.45	0.15	152	0.47	0.31	0.03	95	154.4	47.60	-0.24

Supplementary Table ST2 Relative error (mean μ , standard deviation δ , minimum *Min* and maximum *Max*) in mean concentrations estimated from resampled water quality datasets based on 10,000 Monte Carlo iterations

Determinand	Sampling	HF1				HF2			
		μ	δ	<i>Min</i>	<i>Max</i>	μ	δ	<i>Min</i>	<i>Max</i>
TP (mg ^l ⁻¹)	<i>Daily</i>	0.2	3.7	-16.5	12.1	0.7	3.2	-9.6	10.4
	<i>Weekly</i>	0.3	14.7	-73.7	35.7	0.1	10.1	-63.5	22.2
	<i>Fortnightly</i>	0.3	23.0	-113.7	47.4	-0.1	16.7	-116.2	28.2
	<i>Monthly</i>	1.9	34.4	-254.8	59.7	3.2	26.1	-288.1	42.0
TRP (mg ^l ⁻¹)	<i>Daily</i>	6.6	1.6	-0.5	11.4	0.5	2.1	-7.7	8.6
	<i>Weekly</i>	6.2	5.5	-25.9	21.4	2.0	6.3	-21.1	25.0
	<i>Fortnightly</i>	6.2	8.4	-50.0	30.3	-0.3	10.4	-42.3	34.5
	<i>Monthly</i>	6.6	13.0	-99.4	45.9	5.9	19.7	-55.3	74.8
TURB (NTU)	<i>Daily</i>	4.6	4.2	-19.3	17.1	1.1	5.9	-28.6	15.7
	<i>Weekly</i>	3.2	14.3	-87.0	34.0	-4.7	19.3	-156.2	30.6
	<i>Fortnightly</i>	3.7	20.4	-185.7	39.1	-1.5	29.6	-250.3	44.0
	<i>Monthly</i>	4.2	30.4	-304.8	47.3	0.7	45.1	-440.9	54.6
NO ₃ -N (mg ^l ⁻¹)	<i>Daily</i>	-5.4	0.3	-6.5	-4.4	-0.1	2.4	-8.2	7.5
	<i>Weekly</i>	-5.5	1.3	-11.3	-0.8	-4.7	14.5	-58.2	22.4
	<i>Fortnightly</i>	-5.6	2.0	-13.7	2.7	-1.6	22.3	-85.9	36.9
	<i>Monthly</i>	-5.7	3.2	-21.4	11.1	0.6	34.2	-304.6	48.7
COND/DOC ($\mu\text{Sm}^{-1}/\text{mg}^{-1}$)	<i>Daily</i>	-2.3	0.2	-2.9	-1.6	0.3	0.9	-2.8	4.2
	<i>Weekly</i>	-2.2	0.8	-6.0	0.9	-2.2	4.6	-20.3	13.8
	<i>Fortnightly</i>	-2.3	1.3	-7.5	2.7	0.5	8.5	-31.9	27.3
	<i>Monthly</i>	-2.4	2.0	-11.1	7.0	0.4	12.5	-51.5	32.2

Supplementary Table ST3 Relative error (mean μ , standard deviation δ , minimum *Min* and maximum *Max*) in standard deviation of the concentrations estimated from resampled water quality datasets based on 10,000 Monte Carlo iterations

Determinand	Sampling	HF1				HF2			
		μ	δ	<i>Min</i>	<i>Max</i>	μ	δ	<i>Min</i>	<i>Max</i>
TP (mg ^l ⁻¹)	<i>Daily</i>	0.9	12.0	-50.0	27.5	3.6	24.9	-63.3	47.2
	<i>Weekly</i>	7.0	37.0	-181.4	74.6	17.8	46.5	-208.5	76.8
	<i>Fortnightly</i>	13.8	51.5	-275.9	82.3	21.9	57.8	-357.1	91.5
	<i>Monthly</i>	23.9	63.0	-386.0	90.5	28.0	72.1	-649.7	100.0
TRP (mg ^l ⁻¹)	<i>Daily</i>	4.5	13.9	-71.4	26.2	-0.3	5.1	-18.3	17.9
	<i>Weekly</i>	7.4	28.9	-216.2	43.7	5.7	18.0	-54.3	66.7
	<i>Fortnightly</i>	9.4	35.8	-296.4	53.4	3.8	28.5	-95.6	86.6
	<i>Monthly</i>	13.8	42.4	-466.6	67.7	7.2	53.4	-217.0	100.0
TURB (NTU)	<i>Daily</i>	-6.0	21.7	-134.1	46.6	3.9	23.9	-133.7	46.8
	<i>Weekly</i>	1.6	52.9	-341.2	74.9	12.1	46.4	-373.1	71.9
	<i>Fortnightly</i>	9.2	62.2	-573.9	81.1	18.5	58.0	-521.6	82.3
	<i>Monthly</i>	20.4	75.6	-771.7	86.0	27.1	69.3	-815.3	90.9
NO ₃ -N (mg ^l ⁻¹)	<i>Daily</i>	-1.0	2.9	-12.9	8.5	0.0	7.1	-23.4	18.0
	<i>Weekly</i>	-0.8	10.3	-54.2	26.0	6.2	31.5	-90.0	42.6
	<i>Fortnightly</i>	-0.5	15.1	-94.1	36.3	7.2	42.4	-156.6	52.7
	<i>Monthly</i>	1.0	22.0	-147.2	48.6	10.3	53.4	-299.4	66.6
COND/DOC (μSm ⁻¹ /mg ^l ⁻¹)	<i>Daily</i>	7.0	3.0	-2.6	16.3	0.3	2.7	-9.3	9.0
	<i>Weekly</i>	8.0	12.5	-47.3	38.4	-1.8	10.4	-40.9	35.6
	<i>Fortnightly</i>	9.0	18.3	-83.5	50.6	0.0	19.3	-75.5	61.7
	<i>Monthly</i>	11.2	26.2	-138.7	69.1	-2.8	29.7	-127.0	72.8

Supplementary Table ST4 Relative error (mean μ , standard deviation δ , minimum *Min* and maximum *Max*) in **maximum concentrations** estimated from resampled water quality datasets based on 10,000 Monte Carlo iterations. Minimum error is 0 in all cases as at least one of the resampled datasets contains the absolute maximum value

Determinand	Sampling	HF1				HF2			
		μ	δ	<i>Min</i>	<i>Max</i>	μ	δ	<i>Min</i>	<i>Max</i>
TP (mg ^l ⁻¹)	<i>Daily</i>	39.2	17.6	0.0	61.5	37.3	20.9	0.0	70.7
	<i>Weekly</i>	63.5	17.1	0.0	94.5	64.6	15.0	0.0	80.7
	<i>Fortnightly</i>	74.1	17.7	0.0	96.6	70.2	12.4	0.0	82.9
	<i>Monthly</i>	83.0	15.3	0.0	97.7	75.6	10.1	0.0	88.6
TRP (mg ^l ⁻¹)	<i>Daily</i>	56.0	20.2	0.0	83.7	2.7	2.8	0.0	11.8
	<i>Weekly</i>	78.0	13.3	0.0	91.7	19.7	12.9	0.0	50.0
	<i>Fortnightly</i>	82.6	11.0	0.0	93.8	27.7	13.1	0.0	55.9
	<i>Monthly</i>	86.8	8.4	0.0	95.7	40.6	17.0	0.0	85.3
TURB (NTU)	<i>Daily</i>	61.1	14.7	0.0	89.6	62.5	15.0	0.0	87.4
	<i>Weekly</i>	80.6	13.1	0.0	97.6	81.6	11.1	0.0	94.8
	<i>Fortnightly</i>	86.3	10.8	0.0	98.3	86.5	9.5	0.0	96.5
	<i>Monthly</i>	91.1	9.3	0.0	98.8	90.6	7.7	0.0	97.2
NO ₃ -N (mg ^l ⁻¹)	<i>Daily</i>	38.3	13.6	0.0	52.4	13.0	10.8	0.0	39.8
	<i>Weekly</i>	49.8	7.5	0.0	58.3	59.2	21.7	0.0	79.5
	<i>Fortnightly</i>	52.3	6.4	0.0	60.1	67.9	18.7	0.0	86.8
	<i>Monthly</i>	54.7	5.5	0.0	62.9	76.1	14.9	0.0	90.0
COND/DOC ($\mu\text{Sm}^{-1}/\text{mg}^{-1}$)	<i>Daily</i>	19.2	12.8	0.0	54.1	14.0	8.5	0.0	29.9
	<i>Weekly</i>	45.6	13.8	0.0	61.7	27.5	7.8	0.0	49.2
	<i>Fortnightly</i>	51.7	11.9	0.0	62.5	33.5	9.3	0.0	57.7
	<i>Monthly</i>	56.2	9.8	0.0	63.5	40.1	10.5	0.0	66.0

Supplementary Table ST5 Relative error (mean μ , standard deviation δ , minimum *Min* and maximum *Max*) in 95th percentile of the concentrations estimated from resampled water quality datasets based on 10,000 Monte Carlo iterations

Determinand	Sampling	HF1				HF2			
		μ	δ	<i>Min</i>	<i>Max</i>	μ	δ	<i>Min</i>	<i>Max</i>
TP (mg ^l ⁻¹)	<i>Daily</i>	0.0	6.0	-30.8	18.7	-2.7	6.3	-47.5	16.1
	<i>Weekly</i>	-3.8	24.7	-272.3	44.9	-14.5	44.9	-221.0	35.8
	<i>Fortnightly</i>	-10.8	47.9	-461.0	55.3	0.6	41.4	-233.1	42.9
	<i>Monthly</i>	-35.6	94.9	-885.1	72.1	18.8	33.7	-233.1	61.9
TRP (mg ^l ⁻¹)	<i>Daily</i>	7.9	2.7	-5.6	18.0	-1.8	8.2	-21.7	16.6
	<i>Weekly</i>	6.0	10.1	-49.5	35.7	1.1	14.6	-25.2	37.0
	<i>Fortnightly</i>	5.8	15.0	-132.0	43.8	9.0	16.5	-25.9	44.4
	<i>Monthly</i>	4.5	26.0	-301.8	53.9	25.2	21.5	-25.9	81.5
TURB (NTU)	<i>Daily</i>	-0.6	5.9	-34.4	15.8	1.1	11.1	-76.8	29.2
	<i>Weekly</i>	-5.9	22.6	-203.5	35.4	-22.0	52.2	-533.7	54.4
	<i>Fortnightly</i>	-11.8	39.1	-428.9	46.8	-18.6	81.8	-765.3	68.4
	<i>Monthly</i>	-27.3	75.6	-1375.8	61.4	15.7	69.5	-799.7	74.5
NO ₃ -N (mg ^l ⁻¹)	<i>Daily</i>	-2.9	0.5	-5.2	-0.9	0.8	4.4	-12.6	15.6
	<i>Weekly</i>	-2.9	1.9	-16.4	3.0	-18.0	37.2	-141.9	31.0
	<i>Fortnightly</i>	-3.1	3.2	-30.6	5.8	-21.8	68.9	-272.5	49.0
	<i>Monthly</i>	-3.6	5.9	-64.0	10.6	7.5	57.7	-286.6	61.4
COND/DOC (μSm ⁻¹ /mg ^l ⁻¹)	<i>Daily</i>	-0.9	0.3	-2.3	0.0	0.3	1.8	-4.7	7.3
	<i>Weekly</i>	-0.9	1.1	-9.1	1.9	0.7	7.7	-27.5	26.6
	<i>Fortnightly</i>	-1.1	1.8	-16.4	3.2	3.8	13.2	-44.2	39.0
	<i>Monthly</i>	-1.7	3.6	-38.0	4.1	12.7	15.4	-45.8	50.5

Supplementary Table ST6 Relative error (mean μ , standard deviation δ , minimum *Min* and maximum *Max*) in load estimated from resampled water quality datasets based on 10,000 Monte Carlo iterations

Determinand	Sampling	HF1				HF2			
		μ	δ	<i>Min</i>	<i>Max</i>	μ	δ	<i>Min</i>	<i>Max</i>
TP (mg ^l ⁻¹)	<i>Daily</i>	1.3	18.4	-62.9	43.5	9.4	34.4	-167.5	51.3
	<i>Weekly</i>	10.1	41.2	-196.0	76.1	26.1	30.6	-236.0	64.0
	<i>Fortnightly</i>	17.0	48.0	-266.7	80.7	29.1	30.0	-236.0	64.0
	<i>Monthly</i>	25.7	53.1	-464.4	88.9	32.6	28.8	-236.0	64.0
TRP (mg ^l ⁻¹)	<i>Daily</i>	-2.3	12.0	-46.3	26.8	-3.1	14.1	-86.8	68.0
	<i>Weekly</i>	3.4	28.9	-135.4	48.2	-11.9	28.6	-153.0	91.2
	<i>Fortnightly</i>	7.9	33.6	-162.6	55.6	-19.0	38.7	-153.0	92.6
	<i>Monthly</i>	14.7	37.0	-196.8	69.5	-17.0	45.6	-153.0	92.6
TURB (NTU)	<i>Daily</i>	-4.3	22.7	-121.9	51.8	12.6	44.5	-206.7	72.8
	<i>Weekly</i>	2.4	66.6	-556.1	78.3	40.6	44.9	-307.3	96.8
	<i>Fortnightly</i>	9.8	80.8	-1051.6	83.4	52.4	41.7	-509.3	96.2
	<i>Monthly</i>	22.6	98.0	-1642.3	87.4	60.1	38.8	-313.9	97.3
NO ₃ -N (mg ^l ⁻¹)	<i>Daily</i>	-4.1	3.1	-14.7	9.1	0.0	17.5	-131.8	47.3
	<i>Weekly</i>	-4.7	7.9	-40.0	38.8	7.3	38.3	-359.5	96.6
	<i>Fortnightly</i>	-5.0	10.0	-45.1	55.6	17.6	51.9	-414.7	117.3
	<i>Monthly</i>	-5.3	11.7	-66.4	64.5	29.4	56.8	-414.7	117.3
COND/DOC ($\mu\text{Sm}^{-1}/\text{mg}^{-1}$)	<i>Daily</i>	-1.0	4.1	-13.3	12.1	3.2	10.4	-39.9	40.9
	<i>Weekly</i>	-4.0	11.3	-28.4	33.7	14.2	19.4	-62.1	81.3
	<i>Fortnightly</i>	-6.6	13.9	-34.7	42.4	23.9	23.8	-63.5	81.3
	<i>Monthly</i>	-10.0	15.9	-41.7	50.3	29.3	25.1	-63.5	81.3

Supplementary Table ST7 *c-q* slope calculation (mean μ , standard deviation δ , minimum *Min* and maximum *Max*) from resampled water quality datasets based on 10,000 Monte Carlo iterations

Determinand	Sampling	HF1				HF2			
		μ	δ	<i>Min</i>	<i>Max</i>	μ	δ	<i>Min</i>	<i>Max</i>
TP (mg ^l ⁻¹)	<i>HF</i>	0.36				0.09			
	<i>LF</i>	0.29				-0.09			
	<i>Daily</i>	0.36	0.01	0.30	0.40	0.17	0.05	-0.24	0.42
	<i>Weekly</i>	0.35	0.05	0.15	0.55	0.18	0.32	-0.17	0.78
	<i>Fortnightly</i>	0.36	0.07	0.17	0.69	0.12	0.33	-0.25	0.81
	<i>Monthly</i>	0.42	0.10	0.19	1.03	0.20	0.34	-0.14	0.58
TRP (mg ^l ⁻¹)	<i>HF</i>	0.24				-0.13			
	<i>LF</i>	0.17				-0.20			
	<i>Daily</i>	0.26	0.01	0.22	0.29	-0.20	0.08	-0.81	-0.08
	<i>Weekly</i>	0.26	0.03	0.13	0.41	-0.25	0.48	-0.42	0.52
	<i>Fortnightly</i>	0.27	0.05	0.13	0.52	-0.27	0.76	-0.16	0.93
	<i>Monthly</i>	0.31	0.07	0.16	0.61	1.99	0.95	-0.92	1.63
TURB (NTU)	<i>HF</i>	0.32				0.27			
	<i>LF</i>	0.35				0.36			
	<i>Daily</i>	0.35	0.01	0.31	0.41	0.27	0.04	0.09	0.43
	<i>Weekly</i>	0.35	0.05	0.19	0.54	0.31	0.12	-0.24	0.94
	<i>Fortnightly</i>	0.35	0.07	0.13	0.61	0.33	0.15	-0.64	0.61
	<i>Monthly</i>	0.36	0.10	0.14	0.81	0.30	0.17	-0.75	0.58
NO ₃ -N (mg ^l ⁻¹)	<i>HF</i>	-0.04				0.42			
	<i>LF</i>	0.01				0.30			
	<i>Daily</i>	-0.04	0.01	-0.08	-0.02	0.42	0.05	0.27	0.74
	<i>Weekly</i>	-0.07	0.03	-0.26	0.05	0.49	0.16	0.08	0.49
	<i>Fortnightly</i>	-0.10	0.06	-0.46	0.09	0.55	0.31	0.02	0.75
	<i>Monthly</i>	-0.11	0.12	-0.85	0.32	0.54	0.28	0.12	1.37
COND/DOC ($\mu\text{Sm}^{-1}/\text{mg}^{-1}$)	<i>HF</i>	-0.07				0.11			
	<i>LF</i>	-0.05				0.06			
	<i>Daily</i>	-0.06	0.00	-0.07	-0.04	0.11	0.02	0.05	0.20
	<i>Weekly</i>	-0.06	0.01	-0.10	-0.02	0.15	0.08	-0.08	1.07
	<i>Fortnightly</i>	-0.06	0.02	-0.12	-0.02	0.17	0.29	-0.40	0.37
	<i>Monthly</i>	-0.07	0.02	-0.19	0.03	0.20	0.24	-0.02	0.63

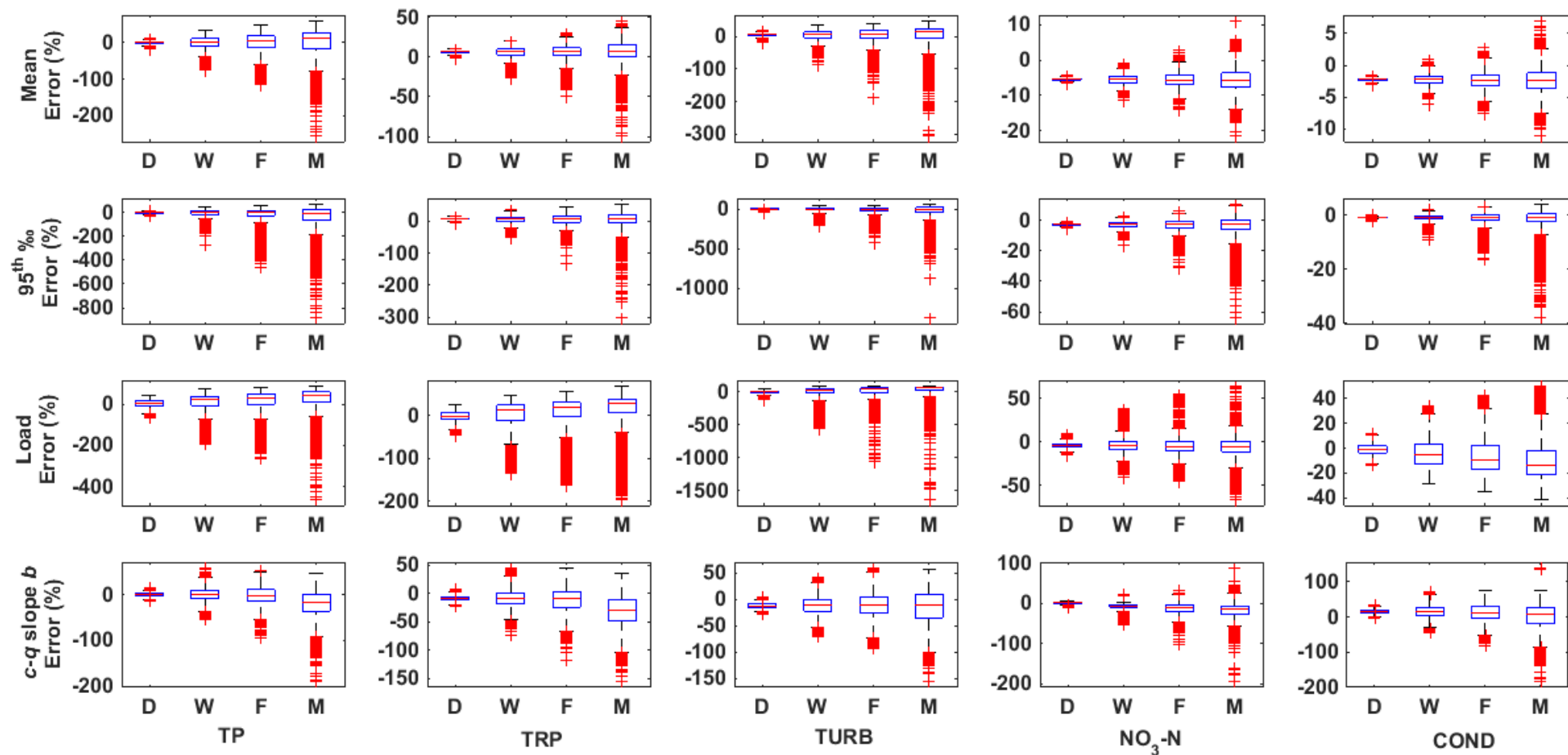
Supplementary Table ST8 Comparison between single linear ($c-q_{Q<}$) and two linear $c-q$ slopes ($c-q_{Q<}$ for flows lower than the threshold value Q and $c-q_{Q>}$ for flows higher than the threshold value Q) for time series showing step changes in the $c-q$ relationship. Slopes which are not significant at 0.05 level are marked with ~~strikethrough~~. Flow-proportional datasets are marked with ^{fp}

Dataset	$c-q_{Q<}$	$c-q_{Q<}$	$c-q_{Q>}$	Q (m^3s^{-1})	Q percentile
TP	$p=0.03$				
SE1	0.11	-0.10	0.53	0.30	44
SE6	0.06	-0.16	0.28	0.10	53
SE9	-0.06	-0.29	0.54	0.31	71
NO5 ^{fp}	0.74	0.75	1.00	0.05	91
NO6 ^{fp}	0.21	-0.05	0.34	0.32	53
UK23	0.29	-0.07	0.22	0.25	40
RP	$p=0.07$				
SE9	-0.16	-0.29	0.31	0.27	71
SE10	0.21	-0.02	0.46	0.10	47
UK7	-0.10	-0.43	0.40	0.63	90
UK13	-0.41	-0.66	0.21	0.30	82
UK36	0.26	-0.16	0.50	0.29	64
SS	$p=0.02$				
NO3 ^{fp}	0.56	0.36	0.73	0.06	77
NO6 ^{fp}	0.54	0.22	0.55	0.30	53
NO9 ^{fp}	0.53	0.36	0.58	0.10	80
UK23	0.90	0.41	0.59	0.31	40
NO₃-N	$p=0.17$				
HF2	0.42	0.10	0.28	0.01	62
SE2	0.62	0.44	0.37	0.28	70
UK16	0.50	0.84	0.00	0.03	22
DOC	-				
HF2	0.11	0.04	0.25	0.01	62
COND	$p=0.10$				
HF1	-0.07	-0.06	-0.26	10.0	98
SE10	-0.18	-0.04	-0.28	0.10	47

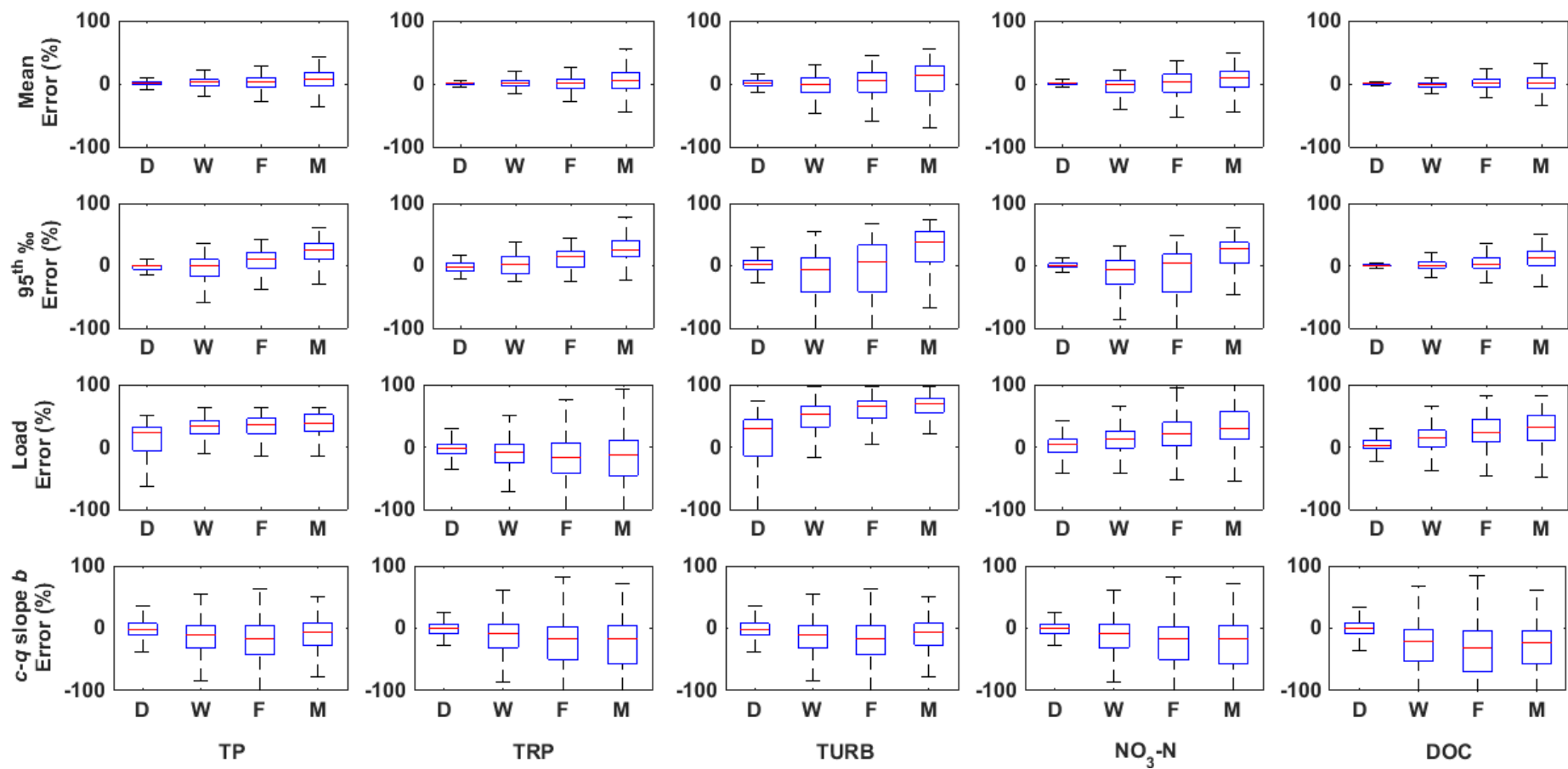
Supplementary Table ST9 Linear trends for flow and water quality time series in the study catchments. An annual change in flow and concentrations is given and expressed in percentage terms (annual change divided by the mean flow/concentration). Annual trends which are not significant at 0.05 level are marked with ~~through~~. Flow-proportional datasets are marked with ^{fp}

Dataset	Q	TP	RP	SS _{LF} TURB _{HF}	NO ₃ -N	DOC	COND
HF1	-9.69	3.18	2.78	8.68	-6.72	-	-2.13
LF1	0.78	0.56	-0.72	1.73	-0.28	-2.26	0.13
HF2	8.30	-2.20	-5.18	4.35	4.86	1.85	-
LF2	-	-2.24	-	5.34	-1.26	-	0.20
SE1	0.53	-0.57	-3.61	2.67	0.45	1.04	-0.45
SE2	1.17	-3.14	0.37	-1.60	-0.95	2.57	-0.11
SE3	0.78	0.56	-0.72	1.73	-0.28	-2.26	0.13
SE4	1.02	0.94	2.72	4.61	-2.95	2.54	-1.46
SE5	-1.27	5.03	2.63	1.05	-3.56	2.29	0.99
SE6	0.77	-4.07	-6.76	-2.34	-2.35	-2.38	0.08
SE7	1.70	-5.00	-5.97	-4.00	-1.22	-2.32	-0.60
SE8	0.52	-0.83	1.02	0.90	-3.20	0.87	-0.89
SE9	0.64	-1.49	-4.24	5.15	-1.42	-10.05	-0.39
SE10	0.00	-1.62	-12.79	4.65	-3.18	-0.74	1.07
SE1 ^{fp}	0.53	3.11	4.83	-0.37	2.44	-2.54	-0.66
SE2 ^{fp}	1.17	3.13	0.23	8.50	0.42	-3.35	1.18
SE3 ^{fp}	0.78	-4.06	-2.96	-10.67	-2.16	-2.48	2.48
SE4 ^{fp}	1.02	0.53	4.97	-7.23	1.11	-5.53	-2.31
SE5 ^{fp}	-1.27	9.46	11.58	5.62	-1.93	-4.96	1.14
SE6 ^{fp}	0.77	4.24	3.84	0.79	0.76	-4.78	1.29
SE7 ^{fp}	1.70	10.50	16.72	1.29	1.60	-2.18	0.22
SE8 ^{fp}	0.52	2.17	-0.76	2.49	0.97	-3.73	0.65
SE9 ^{fp}	0.64	1.21	3.48	-3.27	-2.50	-3.78	1.84
SE10 ^{fp}	0.00	-4.66	0.71	-17.44	-8.00	-2.77	3.70
NO1 ^{fp}	0.13	-0.22	0.29	-4.55	-	-	-
NO2 ^{fp}	-1.94	7.17	3.22	0.49	-1.03	-	-
NO3 ^{fp}	1.04	2.24	0.80	3.74	-0.98	-	-
NO4 ^{fp}	4.74	-2.44	5.75	-17.88	-7.79	-	-
NO5 ^{fp}	1.80	-3.65	1.11	-6.78	-0.35	-	-
NO6 ^{fp}	0.13	1.92	-10.57	2.31	1.12	-	-
NO7 ^{fp}	0.17	-1.81	-15.92	1.89	-0.63	-	-
NO8 ^{fp}	0.72	0.57	2.19	-2.01	-0.33	-	-
NO9 ^{fp}	-1.66	-0.67	-1.64	1.24	-0.65	-	-
NO10 ^{fp}	-1.87	-2.27	-5.23	1.23	-1.49	-	-
UK1	1.40	-	-1.15	-2.75	-3.77	-	2.19
UK2	0.06	-3.25	3.99	6.77	0.51	-	0.53
UK3	1.56	-	-12.93	-7.14	-0.81	-	0.13
UK4	1.28	-	-9.38	0.52	1.15	-	0.86
UK5	0.53	-	-16.84	-	-0.56	-	-2.12
UK6	-0.06	-6.77	-8.38	-3.22	0.14	-	-3.76
UK7	0.17	-	-4.25	-	0.09	-	-
UK8	-0.09	-	-1.48	0.11	-0.73	-	-0.48
UK9	0.68	-	-0.19	-1.28	-0.58	-	-0.33

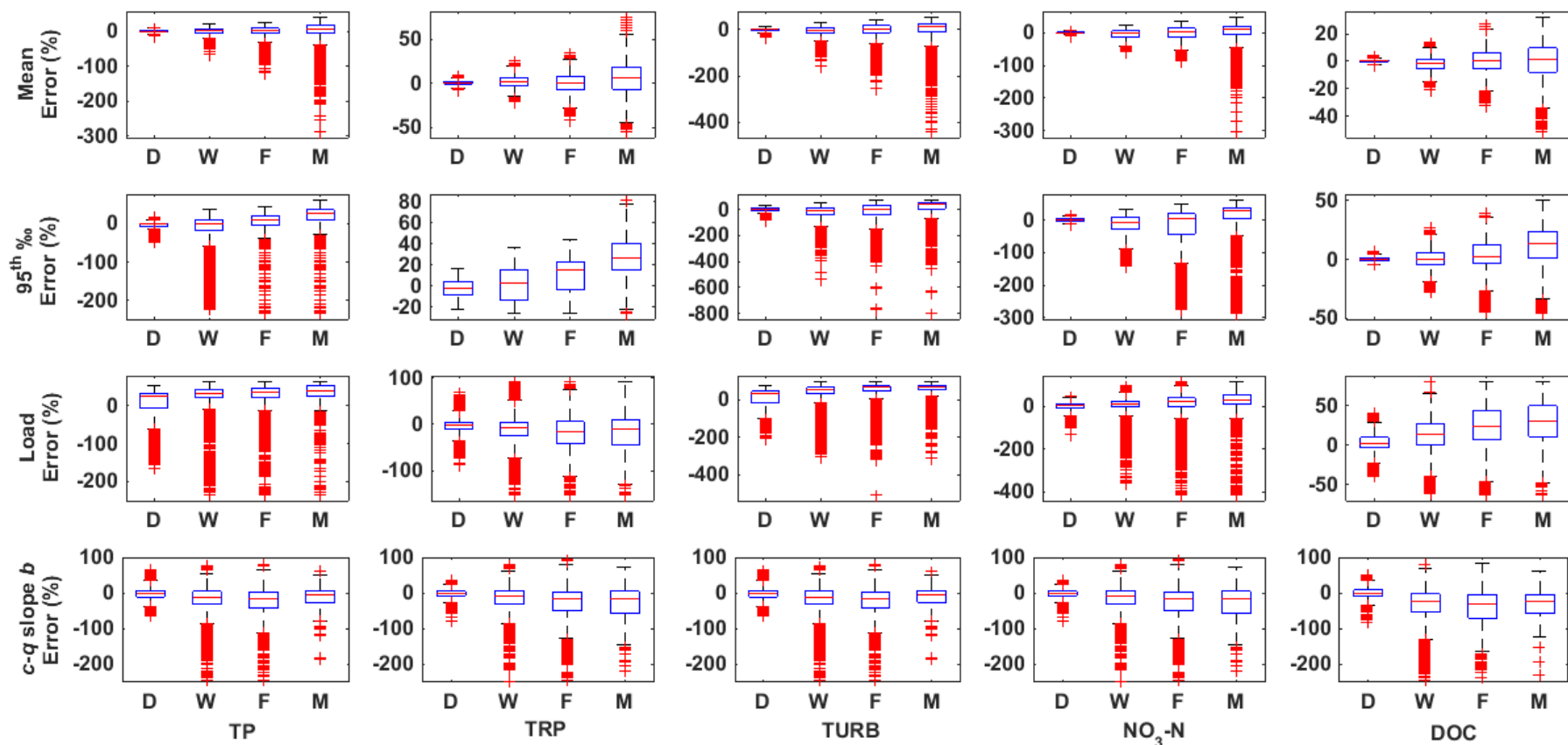
UK10	-0.65	-	-2.28	-	-1.94	-	1.76
UK11	-0.72	0.10	-0.82	-1.59	-1.55	-	0.17
UK12	-1.26	-	-0.02	-3.50	-2.03	-	0.78
UK13	0.82	-	-4.00	-	1.40	-	0.19
UK14	0.40	-	-14.34	-	0.84	-	-2.08
UK15	1.56	-	3.65	28.88	-4.38	-	0.03
UK16	-0.05	-19.39	-3.90	-	-1.49	-	0.19
UK17	-0.11	-	0.18	2.91	-0.19	-	0.28
UK18	0.19	-	1.81	-	2.53	-	0.13
UK19	-0.26	-	-1.25	-	-0.36	-	-0.08
UK20	0.31	-	-0.04	-0.55	0.21	-	0.32
UK21	1.00	-	-13.58	-9.29	-1.20	-	-0.34
UK22	0.50	-3.35	-0.87	-3.14	-3.33	-	0.07
UK23	0.58	-7.00	-0.35	-11.45	-1.83	-	0.11
UK24	0.42	-	-5.50	-3.32	-1.24	-	-0.21
UK25	0.39	-	4.29	-	-3.08	-	0.03
UK26	0.74	-	-1.58	-	-0.37	-	0.02
UK27	0.06	-	-1.69	-	-1.81	-	1.08
UK28	0.64	-	-1.65	-2.22	-0.03	-	0.34
UK29	0.25	-	-0.44	21.83	-1.02	-	0.25
UK30	-0.10	-	-1.09	2.52	-1.41	-	1.21
UK31	0.74	-	-0.22	-149.00	-1.17	-	-1.54
UK32	-0.52	-	-4.56	-0.30	0.40	-	0.11
UK33	0.56	-	-	-	0.87	-	-1.42
UK34	0.97	-3.53	-2.97	-12.09	0.21	-	-0.34
UK35	0.82	-	-1.55	4.90	-3.64	-	8.00
UK36	-0.20	-	0.91	-	-5.84	-	-2.98
UK37	0.10	-	-0.38	-4.78	-1.91	-	1.21
UK38	0.41	-	-1.42	-6.10	-1.38	-	-1.29
UK39	0.79	-	13.47	0.69	3.15	-	0.09
UK40	2.00	-	-	-	-1.28	-	0.65
UK41	0.20	-	9.32	-2.67	-4.33	-	-0.09
UK42	0.15	-	-2.09	7.92	-2.94	-	0.52



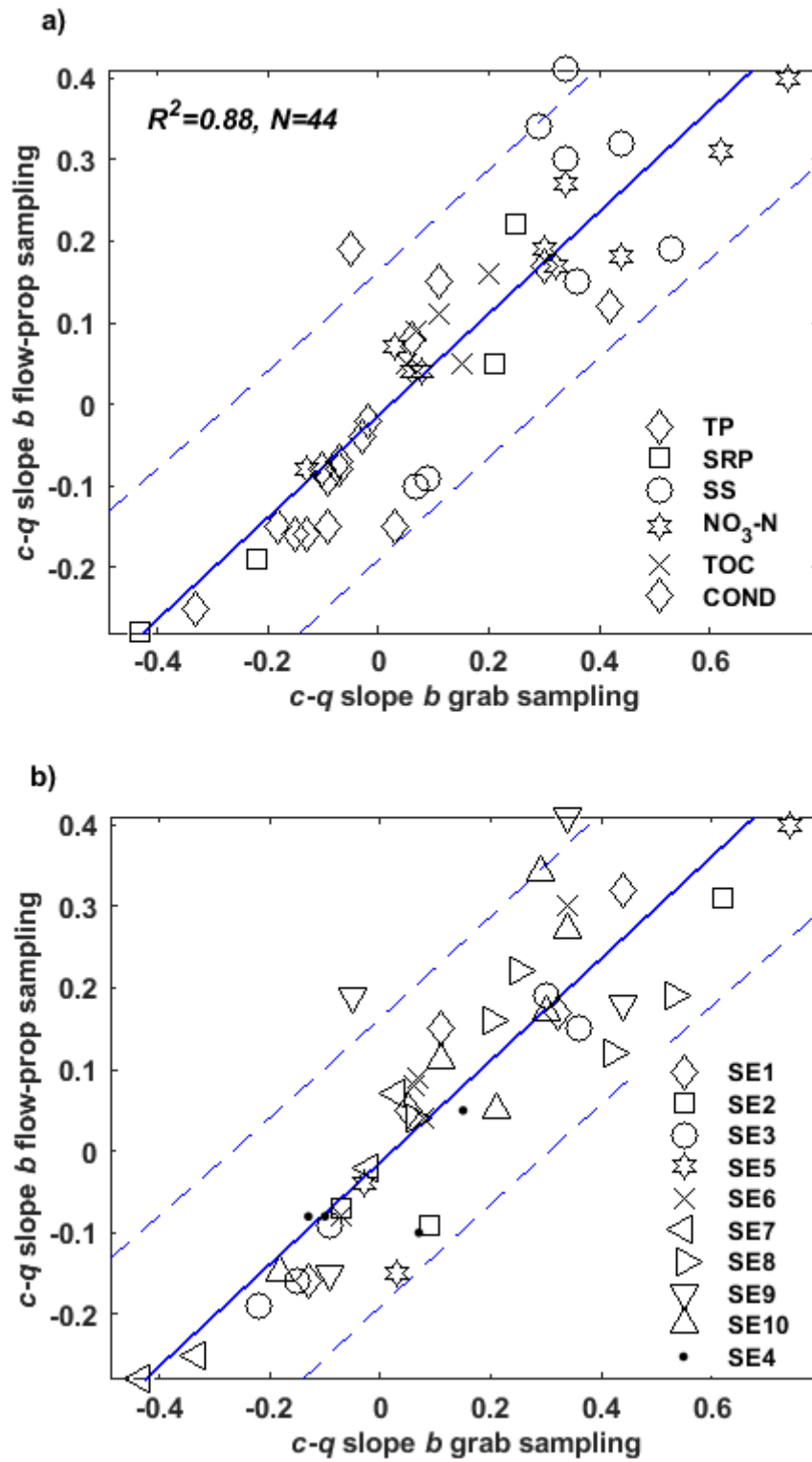
Supplementary Figure SF1 Relative errors in mean (top row), 95th percentile (second row), load estimation (third row) and *c-q* slope (bottom row) for **HF1** for TP, TRP, TURB, NO₃-N and COND. The central red mark is the median, the edges of the box are the 25th and 75th percentiles, the black whiskers extend to the most extreme data points and outliers are plotted as red crosses



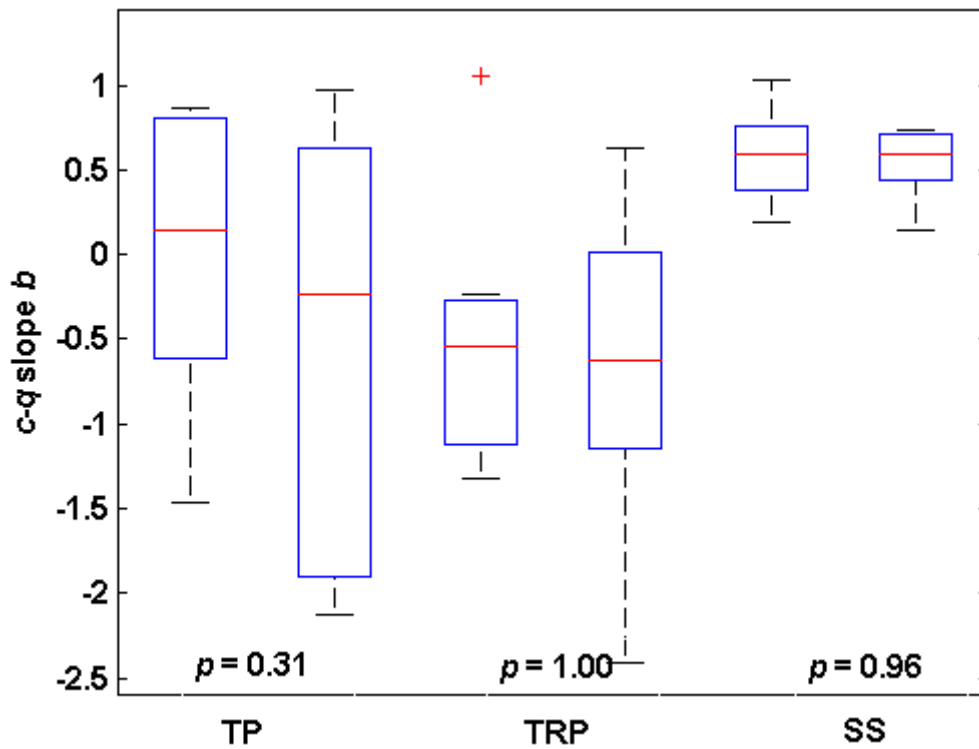
Supplementary Figure SF2 Relative errors in mean (top row), 95th percentile (second row), load estimation (third row) and *c-q* slope (bottom row) for **HF2** for TP, TRP, TURB, NO₃-N and COND. The central red mark is the median, the edges of the box are the 25th and 75th percentiles, the black whiskers extend to the most extreme data points. For better clarity the figure does not contain outliers (given in Supplementary Figure SF3)



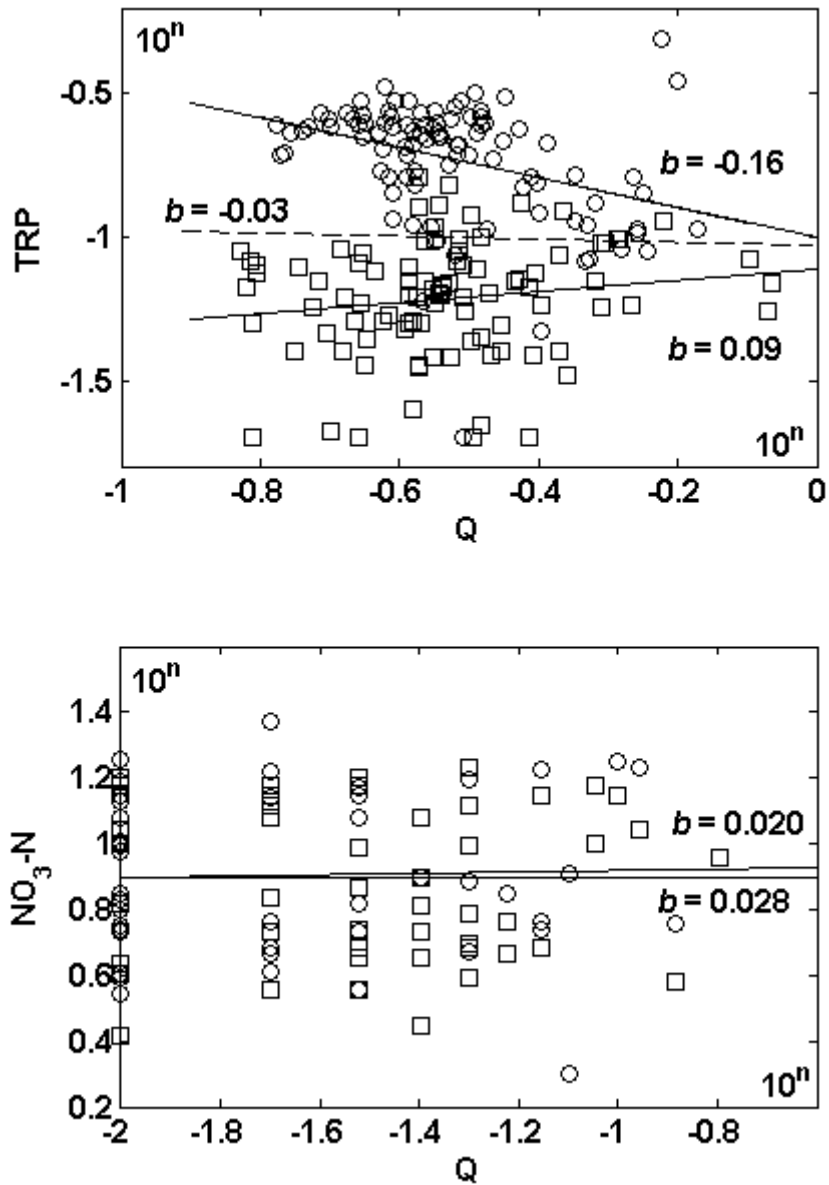
Supplementary Figure SF3 Relative errors in mean (top row), 95th percentile (second row), load estimation (third row) and *c-q* slope (bottom row) for **HF2** for TP, TRP, TURB, NO₃-N and COND. The central red mark is the median, the edges of the box are the 25th and 75th percentiles, the black whiskers extend to the most extreme data points and outliers are plotted as red crosses



Supplementary Figure SF4 Relationship between *c-q* slope *b* calculated from the grab (horizontal axes) and flow-proportional sampling (vertical axes) for determinands (a) and catchments (b)



Supplementary Figure SF5 Analysis of variance (Kruskal-Wallis one-way ANOVA) for the c - q slopes b for annual linear trends $>5\%$. For each determinant datasets showing $>5\%$ linear trends (as in Supplementary Table ST9), were divided into two sub-datasets and c - q slopes were calculated independently for each half. The central red mark is the mean, the edges of the box are the 25th and 75th percentiles, the black whiskers extend to the most extreme data points and outliers are plotted as red crosses



Supplementary Figure SF6 The effect of linear trends on the c - q slopes b for TRP and NO₃-N for the catchments UK6 (top figure) and NO4 (bottom figure). Both determinands for these catchments show significant annual linear trends of -8.38% and -7.79% respectively (Supplementary Table ST9). The time series were split in half (circles for the first half and squares for the second half) and c - q slopes were calculated independently for each half with the best fit line fitted. The dashed line indicates the best fit line fitted to the whole time series. All axes are in logarithmic scale